Made available by Hasselt University Library in https://documentserver.uhasselt.be

Identification, evolution and functional characterization of two Zn CDF-family transporters of the ectomycorrhizal fungus Suillus luteus

Peer-reviewed author version

RUYTINX, Joske; CONINX, Laura; NGUYEN, Hoai; SMISDOM, Nick; Morin, Emmanuelle; Kohler, Annegret; CUYPERS, Ann & COLPAERT, Jan (2017)
Identification, evolution and functional characterization of two Zn CDF-family transporters of the ectomycorrhizal fungus Suillus luteus. In: ENVIRONMENTAL MICROBIOLOGY REPORTS, 9(4), p. 419-427.

DOI: 10.1111/1758-2229.12551
Handle: http://hdl.handle.net/1942/24371

Identification, evolution and functional characterization of two Zn CDF-family transporters of the ectomycorrhizal fungus *Suillus luteus*

Joske Ruytinx[1,*,+], Laura Coninx[1,*], Hoai Nguyen[1], Nick Smisdom[2], Emmanuelle Morin[3], Annegret Kohler[3], Ann Cuypers[1] and Jan V. Colpaert[1]

[1] Hasselt University, Centre for Environmental Sciences, Environmental Biology, Agoralaan building D, 3590 Diepenbeek, Belgium

[2] Hasselt University, Biomedical Research Institute, Agoralaan building C, 3590 Diepenbeek, Belgium

[3] Institut National de la Recherche Agronomique, UMR1136 INRA-Université de Lorraine Interactions Arbres/Microorganismes, Laboratoire d'Excellence ARBRE, 54280 Champenoux, France

* equally contributed to this work

[+] For correspondence:

joske.ruytinx@uhasselt.be; phone: +32 11 268377; fax: +32 11 268301

Running title: Identification and characterization of two Zn transporters

Summary

Two genes, *SlZnT1* and *SlZnT2*, encoding Cation Diffusion Facilitator (CDF) family transporters were isolated from *Suillus luteus* mycelium by genome walking. Both gene models are very similar and phylogenetic analysis indicates that they are most likely the result of a recent gene duplication event. Comparative sequence analysis of the deduced proteins predicts them to be Zn transporters. This function was confirmed by functional analysis in yeast for *SlZnT1*. SlZnT1 was able to restore growth of the highly Zn sensitive yeast mutant Δzrc1 and localized to the vacuolar membrane. Transformation of Δzrc1 yeast cells with *SlZnT1* resulted in an increased accumulation of Zn compared to empty vector transformed Δzrc1 yeast cells and equals Zn accumulation in wild type yeast cells. We were not able to express functional SlZnT2 in yeast. In *S. luteus*, both *SlZnT* genes are constitutively expressed whatever the external Zn concentrations. A labile Zn pool was detected in the vacuoles of *S. luteus* free-living mycelium. Therefore we conclude that *SlZnT1* is indispensable for maintenance of Zn homeostasis by transporting excess Zn into the vacuole.

Keywords

Zinc transporter, *Suillus luteus*, Zinc detoxification, Zinc storage, Cation Diffusion Facilitator

Introduction

Zinc (Zn) is an essential micronutrient as it is involved as co-factor, structural or signalling element in a wide range of cellular processes (Eide, 2009). Nevertheless, it becomes toxic when present in excess. The cellular Zn concentration of healthy, well-functioning cells ranges from 0.1 - 0.5 mM. Most of the cellular Zn is bound to proteins and the labile/free fraction is only in the nano to picomolar range (Eide, 2006; Simm *et al.*, 2007). To assure cellular homeostasis in situations of Zn limitation as well as Zn surplus, all organisms require a system to fine-tune Zn availability in the cell. This system is well studied in yeast and mammals (Sekler *et al.*, 2007; North *et al.*, 2012) and is mainly relying on transporters. In all eukaryotic cells, ZIP (Zrt-, Irt-like proteins) and CDF (cation diffusion facilitator) families of transporters account for most of the Zn transport across membranes. ZIP transporters mediate Zn transport towards the cytoplasm. They are involved in Zn uptake from the extracellular space (environment) and remobilization from organelles (Kambe *et al.*, 2006). CDF transporters remove Zn from the cytoplasm. Members of this family of transporters move Zn to the extracellular space or into cellular compartments and therefore are involved in Zn export and storage (Montanini *et al.*, 2007). However, ZIP and CDF family transporters are not restricted to the transport of Zn. Both families enclose Zn, Fe and Mn transporters and several of them are able to transport Cd in an unspecific way (Guerinot, 2000; Montanini *et al.*, 2007). Substrate specificity of CDF family transporters can be predicted by phylogenetic analysis that classifies CDF family transporters into three major groups, of which the characterized members share the same metal specificity. Metal specificity of a newly identified member can be inferred by its phylogenetic position in one of the three major groups (Montanini *et al.*, 2007). Until now, metal specificity of ZIP transporters cannot be predicted unambiguously from protein sequence only.

Mycorrhizal fungi are mutualists living in symbiosis with plant roots. They provide their host plant with essential low-bioavailable nutrients as nitrogen and phosphorus in exchange for photosynthesis-derived sugar (Smith & Read, 2008). Besides, this mutualism results in other benefits for the host plant including protection from heavy metal stress. Mitigation of toxic effects in plants by mycorrhizal fungi when grown in Zn-contaminated soils is well-documented (Adriaenssen et al., 2004; Ferrol et al., 2016). Nevertheless, molecular mechanisms of cellular Zn homeostasis in mycorrhizal fungi are not well-characterized and their impact on plant nutrient balances is poorly understood. Detoxification of excess Zn in mycorrhizal fungi includes storage in subcellular compartments. The ectomycorrhizal (ECM) fungus *Suillus bovinus* stores excess Zn in vacuoles (Ruytinx et al., 2013); *Hebeloma cylindrosporum*, another ECM fungus in ER-derived vesicles (Blaudez & Chalot, 2011). In *H. cylindrosporum* a CDF family transporter HcZnT1, localized at the ER-membrane, is most likely involved in the transport of cytoplasmic Zn towards the ER. A similar transporter was characterized in the ericoid mycorrhizal (ERM) fungus *Oidiodendron maius* (Khouja et al., 2013). RaCDF1 of *Russula atropurpurea* (ECM) clusters in phylogenetic analysis close to HcZnT1 and OmZnT1, confers Zn tolerance to Zn sensitive yeast mutants but localizes on the tonoplast and is likely involved in vacuolar Zn storage. A second transporter of the same family, RaCDF2 was identified in this Zn-accumulating ectomycorrhizal fungus. RaCDF2 is closely related to Mn transporting CDF's, localizes to the plasma membrane when heterologous expressed in yeast, does not confer Mn tolerance to Mn sensitive yeast mutants and likely acts as a bidirectional transporter of Zn, Cd and Co (Sacky et al., 2016). In arbuscular mycorrhizal (AM) fungi *GintZnT1* of *Rhizophagus intraradices* was identified and predicted to be a vacuolar Zn transporter of the CDF-family (Gonzalez-Guerrero et al., 2005). Here we localize the labile Zn pool of *S. luteus* and report the functional characterization of two CDF-family transporters. *S. luteus* is a cosmopolitan ectomycorrhizal fungus, associated

with pine trees. In particular, in primary successions of pines this species is abundant and involved in seedling establishment (Hayward et al., 2015). On severely metal-contaminated sites, Zn-tolerant *S. luteus* populations evolved and protect their host tree effectively from Zn toxicity (Adriaensen et al., 2004; Colpaert et al., 2011). The *Suillus-Pinus* association has a high potential for use in bio-stabilisation and restoration of metal-disturbed sites. However, fundamental knowledge on the molecular mechanisms involved in metal homeostasis in the plant and fungal partner is required to select most suited ecotypes and to fully exploit this potential.

Results and discussion

Localization of labile Zn pool in *S. luteus*

All fungi store excess Zn in a specific organelle where it is no longer able to harm the cell and from where it can be remobilised in case of deficiency. For most fungi the vacuole is the main site for Zn storage (Gonzalez-Guerrero *et al.*, 2008; Ott *et al.*, 2002; Simm *et al.*, 2007). On the other hand, some fungi have special ER related vesicles (or zincosomes) for Zn storage (Clemens *et al.*, 2002; Blaudez & Chalot 2011). Subcellular labeling of Zn in *S. luteus* mycelium was performed with a fluorescent marker for free Zn^{2+}, FluoZin3 (Molecular Probes, Invitrogen), which is able to detect free Zn^{2+} in the 1-100 nM range. A fluorescence pattern, clearly indicating vacuoles, was observed (Fig. 1). Hyphae containing vacuoles with labile Zn were distributed all over the mycelium (Fig. 1 a-c). External Zn concentration did not change the observed fluorescence pattern, only intensity of the fluorescence changed. *S. luteus* clearly stores Zn into the vacuole. No other accumulation pattern was detected despite of different external Zn concentrations. Therefore vacuolar Zn storage is expected to be one of the mechanisms to detoxify Zn and to maintain homeostasis in case of excess Zn in *S. luteus*.

Identification and evolutionary origin of two *S. luteus* transporters of the CDF family

CDF family transporters are often involved in Zn storage in vacuoles or ER related vesicles in fungi. These transporters are key elements of the Zn homeostatic network of eukaryotes (Montanini *et al.*, 2007; Kambe *et al.*, 2008; Gustin *et al.*, 2011). By removing Zn from the cytosol they are particularly important in the prevention from Zn toxicity (Gaither & Eide, 2001). Using a genome walking approach targeting vacuolar Zn transporters of the CDF family we picked up two *S. luteus* gene fragments. Further analysis by genome walking and RACE protocols revealed that those fragments belong to the genes encoding proteins with protein ID 807028 and 814105 in the JGI *S. luteus* genome database. The genes were named *SlZnT1* and *SlZnT2* and both gene models are very alike (Supplemental figure S1). They consist of 9 exons interspersed with introns of +/- 50 nucleotides. *In silico* translations of full length cDNA's (1623 and 1516 bp) identified open reading frames of 1320 and 1362 bp encoding a 440 and 453 amino acid-long polypeptide respectively (Fig. 2). A high percentage of sequence identity (85%) between both predicted proteins is observed. The predicted proteins show sequence and structural features typical of CDF family transporters.

CDF transporters are characterized by six transmembrane domains and a histidine rich motif $(HX)_n$ in the cytosolic loop between transmembrane helices IV and V. For most proteins of this transporter family the histidine rich motif is located directly after helix IV and contains three to six HX repeats (Gaither & Eide, 2001). The topology prediction program TMHMM predicted 6 transmembrane domains for both deduced *S. luteus* proteins. The deduced proteins are very similar but show a considerable level of sequence diversification in the cytosolic loop between helix IV and V (Fig. 2). *SlZnT1* is with its predicted six transmembrane domains and $(HX)_3$ domain a typical CDF family member. SlZnT2 is somewhat aberrant since the normal $(HX)_n$ motif shows seven repeats and an extra, second $(HX)_n$ motif (n=5) is present just before helix V. The exact function of the $(HX)_n$ motif is unclear but it is expected to have a role in metal recruitment (Gaither & Eide, 2001). In plants the histidine-rich loop is hypothesized to

play a role as a Zn chaperone to determine the identity of the transported ions (Podar et al., 2012). The atypical sequence of SlZnT2 with the presence of an additional $(HX)_n$ motif might therefore have some implications for metal selectivity and specificity. However, Lin *et al.* (2009) showed that metal specificity is determined by a cooperation between transmembrane domain II and V. Several single amino acid substitutions within transmembrane helices II and V of the S. *cerevisiae* vacuolar Zn transporter *ZRC1* resulted in an Fe and Mn transporting protein. Some of these proteinscreated by site directed mutagenesis retained the ability to transport Zn, others not (Lin *et al.*, 2008; Lin *et al.*, 2009). In particular the amino acid located four residues before the highly conserved aspartate (D) in transmembrane domain II and V is very important in metal selectivity (Montanini *et al.*, 2007). Both identified *S. luteus* transporters have a HXXXD motif in transmembrane helices II and V, a feature specific for the group of Zn transporting CDFs (Fig. 2).

Comparisons with the NCBI nr protein sequences (BLASTx) or fungal protein models at jgi MycoCosm resulted in the same hits for SlZnT1 and SlZnT2. However, ranking of the hits is different. Previously characterized CDF family transporters with the highest sequence identity are the RaCDF1 protein of *Russula atropurpurea* (53%) and the GintZnT1 protein of *Rhizophagus intraradices* (44%) for SlZnT1 and SlZnT2, respectively. All hits are protein models corresponding to CDF family transporters. Remarkable is that only species from the suborder *Suillineae* and *Coniophora puteana* occur twice in the list of BLASTx hits. To elucidate the origin and relationship of SlZnT1 and SlZnT2 a neighbour-joining (NJ) tree was built using previously characterized fungal CDF family transporters and BLASTx hits. In this tree (Fig. 3) both SlZnT1 and SlZnT2 cluster to the Zrc1/Cot1-like Zn-CDFs (Montanini *et al.* 2007). Within the cluster of Zrc1/Cot1-like CDFs, SlZnT1 clusters with the majority of the BLASTx hits while SlZnT2 divaricates earlier and groups in a cluster that only contains sequences of species that had two BLASTx hits. Reconciliation of the tree with an ITS

phylogeny of the considered taxa supports a gene duplication in the common ancestor of Suillineae and the Coniophora/Serpula clade (supplemental figure S2). Gene expansion and loss are common events in fungal genome evolution and may result in phenotypic alterations (Floudas *et al.*, 2012, Kohler et al., 2015). Interestingly, *S. luteus* and some other species within the Suillineae clade are known to evolve Zn-tolerant phenotypes on severely metal-contaminated soils (Colpaert *et al.*, 2004). Members of the SlZnT2 cluster could therefore be candidate genes to study in adaptive Zn tolerance of Suilloid fungi. Five additional *S. luteus* genes predicted to encode CDF transporters were identified and cluster within different clusters of the phylogenetic tree (Fig.3 and Supplemental figure S3).

Functional characterization of *SlZnT1* in yeast

SlZnT1 was expressed in yeast to confirm the functionality predicted by comparative sequence analysis. Heterologous expression in the eukaryotic model system *S. cerevisiae* is a common strategy to get insight into gene function (Osborn & Miller, 2007; Mokdad-Gargouri *et al.*, 2012). By comparative gene analysis, *SlZnT1* is predicted to encode a vacuolar Zn transporter. *SlZnT1* gene product was able to partly restore growth of Δzrc1, a yeast mutant defective in vacuolar Zn storage and highly sensitive for Zn, on Zn enriched medium (Fig. 4). The highly sensitive phenotype of Δcot1 (defective vacuolar CDF transporter) on cobalt (Co) containing medium could not be restored by the identified *S. luteus* gene product. Also, the defective vacuolar ATP (adenosine triphosphate) binding cassette of Δycf1 (Cd sensitive) yeast and the defective golgi P-type ATPase of Δpmr1 (Mn sensitive) yeast could not be complemented by SlZnT1 (Supplementary figure S4).

To better understand the role of *SlZnT1* in Zn homeostasis the cellular metal content of wild type yeast (+ empty vector (EV)), Δzrc1 (+EV) and Δzrc1 carrying *SlZnT1* was determined after exposure to Zn. All yeast cultures showed an increased Zn content after growing in Zn enriched medium (Supplemental fig. S6). Wild type yeast and Δzrc1 yeast containing *SlZnT1*

accumulated a comparable amount of Zn. This amount is significantly higher than the amount measured in Δzrc1. No significant differences in Fe and Mn content were observed among the yeast mutants when exposed to Zn (Supplementary figure S7), indicating the Zn specificity of the transporter. Translational fusion of SlZnT1 to GFP confirmed its vacuolar localization in yeast (Fig. 5). Yeast cells containing the SlZnT1::EGFP fusion construct showed a bright green GFP fluorescent ring at the level of the vacuolar membrane (Fig. 5a-d). Clear co-localisation of the GFP fluorescence with the red fluorescence of the tonoplast specific staining FM4-64 was observed for the SlZnT1::EGFP fusion construct.

All together our observations support a ZRC1-like function for SlZnT1. ZRC1 is involved in vacuolar Zn storage and largely determines yeast's ability to detoxify excess Zn (Kamizono et al., 1989). Most likely, SlZnT1 has a role in cellular Zn homeostasis in *S. luteus* by transporting excess Zn towards the vacuolar stock.

Functional characterization of *SlZnT2* in yeast

Although *SlZnT1* and *SlZnT2* are very similar, we were not able to express functional *SlZnT2* in *S. cerevisiae*. None of metal sensitive phenotypes of the tested yeast mutants defective in metal transport could be complemented by expression of *SlZnT2* (Fig. 4 and supplemental figure S4). Though, the gene is clearly expressed since *SlZnT2* transcript could be detected in the transformed yeast cells by PCR (Supplementary figure S5). Translational fusion to GFP resulted in accumulation of GFP inside the vacuole (Fig. 5). Fusion of the EGFP protein to SlZnT2 resulted in a green fluorescent vacuolar content when expressed in yeast for both N-terminal and C-terminal fusion. Figure 5 (e-g) shows that EGFP fluorescence is nicely surrounded by FM4-64 fluorescence. Zn content of Δzrc1 containing *SlZnT2* was similar to that of Δzrc1 containing the empty vector and is significantly lower than in WT yeast cells exposed to the same external Zn concentration (Supplemental fig. S6).

Heterologous expression is a powerful way to study gene function but has some limitations because of differences in e.g. codon usage, posttranscriptional regulation, posttranslational modifications and protein targeting signals (Yin *et al.*, 2007; Mattanovich *et al.*, 2012). These differences might be at the basis of the non-functioning of SlZnT2 in yeast. The functional characterization of the *R. intraradices* CDF transporter GintZnT1 in yeast resulted in similar problems. Although, GintZnT1 could be detected by western blotting in transformed cells, it was not able to complement any metal sensitive yeast mutants. This transporter could not be affiliated to a specific membrane; the expressed protein seemed to accumulate all over the cytoplasm (Gonzalez-Guerrero *et al.*, 2005). However, the exact reason of non-functioning is probably different for both proteins since they accumulate in different cellular compartments in yeast. Regulation of posttranslational modifications and protein targeting are only little explored in mycorrhizal fungi and deserve further attention.

SlZnT1 and _SlZnT2_ gene expression in _S. luteus_

Gene expression levels of *SlZnT1* and *SlZnT2* were determined in *S. luteus* after 48h exposure to different concentrations of Zn, including concentrations inducing cellular Zn deficiency and toxicity. Figure 6a and 6b show that both *SlZnT1* and *SlZnT2* expression were constitutive. Neither exposure to excess Zn, nor limiting Zn changed the expression level of the transporters when compared to the control condition (20µM Zn). On average *SlZnT1* and *SlZnT2* expression level differ by at least a factor five, with *SlZnT2* showing the lowest transcript abundance (Fig. 6a and 6b). Insensitivity of gene expression for high external Zn concentrations was demonstrated previously for the Zn CDF transporter *ZRC1* of *S. cerevisiae* (MacDiarmid *et al.*, 2003) and *HcZnT1* of *Hebeloma cylindrosporum* (Blaudez & Chalot, 2011). However, in *R. intraradices* gene expression of the *SlZnT* homologous gene *GintZnT1* is transiently induced by elevated external Zn concentrations (Gonzalez-Guerrero *et al.*, 2005). *S. cerevisiae* cells show a proactive strategy of homeostatic regulation of free cellular

Zn content by an induction of *ZRC1* gene expression in Zn limited cells (MacDiarmid *et al.*, 2003). Being proactive guarantees a rapid resistance in case of repletion. In *S. luteus* no change in SlZnT gene expression level was detected after growth without Zn for 48h (Fig. 6). This might imply that both SlZnT's are not regulated proactive neither reactive by external Zn concentration at the transcriptional level.

Conclusion

SlZnT1 probably has a key role in vacuolar Zn storage in *S. luteus* considering the results obtained by heterologous expression in yeast. Based on the phylogenetic analysis it is likely that *SlZnT2* is involved in vacuolar Zn storage as well. However, redundancy caused by gene duplication might lead to diversification and neo-functionalization (Assis & Bachtrog, 2013). Subcellular targeting of SlZnT2 is unclear and vacuolar localisation was not confirmed. This protein might have evolved to transport Zn out of the cell by localisation to the plasma membrane or ER. Since we could never observe a zincosomes related accumulation pattern in *S. luteus*, a role for *SlZnT2* in Zn detoxification by storage or secretion via zincosomes is rather unlikely unless Zn is tightly bound to a chelator, preventing its detection by the fluorescent marker. Also, Zn specificity of SlZnT2 was not confirmed and comparative sequence analyses are not always conclusive. RaCDF2 of *Russula atropurpurea* is a Zn exporting plasma membrane transporter nested within a cluster of Mn transporters and without the Zn-specific HXXXD motif in transmembrane helices II and V (Sacky et al., 2016). CDFs are conserved proteins and this kind of changes in metal specificity seem rather exceptional since all other previously characterized CDFs of Bacteria, Plants and Animals cluster in phylogenetic trees according to the metal they are transporting (Montanini et al., 2007; Cubillas et al., 2013). A role of SlZnT2 in Zn transport and homeostasis of *S. luteus* is likely. Other *S. luteus* genes are predicted to function in Fe and Mn transport. Five additional CDF-encoding genes were identified in the *S. luteus* genome (Fig. 3 and Supplemental figure

S3). These genes need to be further characterized to confirm their putative role and understand their contribution in Zn, Fe and Mn homeostasis of *S. luteus*.

Acknowledgements

We greatly acknowledge Carine Put, Pieter Ceyssens and Bram Vanhumbeeck for technical assistance. This research was financially supported by the Research Foundation – Flanders (FWO-project G.0925.10 and G.0792.13) and a Methusalem project (08M03).

Competing interest

The authors declare that they have no competing interest

References

Adriaensen, K., van der Lelie, D., Van Laere, A., Vangronsveld, J., Colpaert, J.V. (2004) A zinc-adapted fungus protects pines from zinc stress. New Phytol 161(2): 549-555.

Assis, R., Bachtrog, D. (2013) Neofunctionalization of young duplicate genes in Drosophila. Proc Natl Acad Sci USA 110: 17409-17414.

Blaudez, D., Chalot, M. (2011) Characterization of the ER-located zinc transporter ZnT1 and identification of a vesicular zinc storage compartment in *Hebeloma cylindrosporum*. Fungal Genet Biol 48: 496-503.

Clemens, S., Bloss, T., Vess, C., Neumann, D., Nies, D.H., Zur Nieden, U. (2002) A transporter in the endoplasmic reticulum of *Schizosaccharomyces pombe* cells mediates zinc storage and differentially affects transition metal tolerance. J Biol Chem 277: 18215-18221.

Colpaert, J.V., Muller, L.A.H., Lambaerts, M., Adriaensen, K., Vangronsveld, J. (2004) Evolutionary adaptation to Zn toxicity in populations of Suilloid fungi. New Phytol 162: 546-559.

Colpaert, J.V., Wevers, J.H.L., Krznaric, E., Adriaensen, K. (2011) How metal-tolerant ecotypes of ectomycorrhizal fungi protect plants from heavy metal pollution. Annals of Forest Science 68:17–24.

Cubillas, C., Vimiesa, P., Tabche, M.L., Garcia-de los Santos, A. (2013) Phylogenomic analysis of cation diffusion facilitator proteins uncovers Ni^{2+}/Co^{2+} transporters. Metallomics 5: 1634-1643.

Eide, D.J. (2006) Zinc transporters and the cellular trafficking of zinc. Biochim Biophys Acta 1763: 711-722.

Eide, D.J. (2009) Homeostatic and adaptive responses to zinc deficiency in *Saccharomyces cerevisiae.* J Biol Chem 284: 18565-18569.

295 Ferrol, N., Tamayo, E., Vargas, P. (2016) The heavy metal paradox in arbuscular
296 mycorrhizas: from mechanisms to biotechnological applications. J Exp Bot 67:6253-
297 6265.
298 Floudas, D., Binder, M., Riley, R., Barry, K., Blanchette, R.A., Henrissat, B., Martinez, A.T.,
299 Otillar, R., Spatafora, J.W., Yadav, J.S. *et al.* 2012. The Paleozoic origin of enzymatic
300 lignin decomposition reconstructed from 31 fungal genomes. Science 336: 1715-1719.
301 Gaither, L.A., Eide, D.J. (2001) Eukaryotic zinc transporters and their regulation. Biometals
302 14(3-4): 251-270.
303 Gonzalez-Guerrero, M., Azcon-Aguilar, C., Mooney, M., Valderas, A., MacDiarmid, C.W.,
304 Eide, D.J., Ferrol, N. (2005). Characterization of a *Glomus intraradices* gene encoding
305 a putative Zn transporter of the cation diffusion facilitator family. Fungal Genet Biol
306 42: 130-140.
307 Gonzalez-Guerrero, M., Melville, L.H., Ferrol, N., Lott, J.N.A., Azcon-Aguilar, C., Peterson,
308 R.L. (2008) Ultrastructural localization of heavy metals in the extraradical mycelium
309 and spores of the arbuscular mycorrhizal fungus *Glomus intraradices.* Can J Microbiol
310 54: 103-110.
311 Guerinot, M.L. (2000). The ZIP family of metal transporters. Biochim Biophys Acta 1465:
312 190-198.
313 Gustin, J., Zanis, M., Salt, D. (2011) Structure and evolution of the plant cation diffusion
314 facilitator family of ion transporters. BMC Evol Biol 11: 76.
315 Hayward, J., Horton, T.R., Pauchard, A., Nuñez, M.A. (2015) A single ectomycorrhizal
316 fungal species can enable a *Pinus* invasion. Ecology 96: 1438-1444.
317 Kambe, T., Suzuki, T., Nagao, M., Yamaguchi-Iwai, Y. (2006) Sequence similarity and
318 functional relationship among eukaryotic ZIP and CDF transporters. Genomic
319 Proteomic Bioinformatic 4(1): 1-9.

Kambe, T., Weaver, B., Andrews, S. (2008) The genetics of essential metal homeostasis during development. Genesis 46: 214-228.

Kamizono, A., Nishizawa, M., Teranishi, Y., Murata, K., Kimura, A. (1989) Identification of a gene conferring resistance to zinc and cadmium ions in the yeast *Saccharomyces cerevisiae.* Mol Gen Genet 219: 161-167.

Khouja, H.R., Abba, S., Lacercat-Didier, L., Daghino, S., Doillon D., Richaud, P., Martino, E., Vallino M., Perotto S., Chalot, M., Blaudez D. (2013) OmZnT1 and OmFET, two metal transporters from the metal-tolerant strain Zn of the ericoid mycorrhizal fungus Oidiodendron maius, confer zinc tolerance in yeast. Fungal Genetics and Biology 52:53-64.

Kohler, A., Kuo, A., Nagy, L.G., Morin, E., Barry, K.W., Buscot, F. et al. (2015) Convergent losses of decay mechanisms and rapid turnover of symbiosis genes in mycorrhizal mutualists. Nat Genet 47: 410-415.

Lin, H., Kumanovics, A., Nelson, J.M., Warner, D.E., Ward, D.M., Kaplan, J. (2008). A single amino acid change in yeast vacuolar metal transporters ZRC1 and COT1 alters their substrate specificity. J Biol Chem 283: 33865-33873.

Lin, H., Burton, D., Li, L., Warner, D.E., Philips, J.D., Ward, D.M., Kaplan, J. (2009) Gain of function mutants identify amino acids within transmembrane domains of the yeast vacuolar transporter Zrc1 that determine metal specificity. Biochem *J* 422: 273-283.

MacDiarmid, C.W., Milanick, M.A., Eide, D.J. (2003) Induction of the ZRC1 metal tolerance gene in zinc-limited yeast confers resistance to zinc shock. J Biol Chem 278: 15065-15072.

Mattanovich, D., Branduardi, P., Dato, L., Gasser, B., Sauer, M., Porro, D. (2012) Recombinant protein production in yeast. Method Mol Biol 824: 329-359.

344 Mokdad-Gargouri, R., Abdelmoula-Soussi, S., Hadiji-Abbès, N., Amor, I.Y., Borchani-
345 Chabchoub, I., Gargouri, A. (2012) Yeasts as a tool for heterologous gene expression.
346 Method Mol Biol 824: 359-370.
347 Montanini, B., Blaudez, D., Jeandroz, S., Sanders, D., Chalot, M. (2007) Phylogenetic and
348 functional analysis of the cation diffusion facilitator (CDF) family: improved signature
349 and prediction of substrate specificity. BMC Genomic 8: 107-122.
350 North, M., Steffen, J., Longuinov, A., Zimmerman, G., Vulpe, C., Eide, D. (2012) Genome-
351 wide functional profiling identifies genes and processes important for zinc limited
352 growth of *Saccharomyces cerevisiae.* PLOS Genet 8(6): e1002699.
353 Osborn, M.J., Miller, J.R. (2007) Rescuing yeast mutants with human genes. Brief Funct
354 Genomic Proteomic 6: 104-111.
355 Ott, T., Fritz, E., Polle, A., Schützendübel, A. (2002) Characterization of antioxidative
356 systems in the ectomycorrhiza-building basidiomycete *Paxillus involutus* (Bartsch) Fr.
357 and its reaction to cadmium. FEMS Microbiol Ecol 42: 359-366.
358 Podar, D., Scherer, J., Noordally, Z., Herzijk, P., Nies, D., Sanders, D. (2012) Metal
359 selectivity determinants in a family of transition metal transporters. J Biol Chem 287:
360 3185-3196.
361 Ruytinx, J., Nguyen, N., Van Hees, M., Op De Beeck, M., Vangronsveld, J., Carleer, R.,
362 Colpaert, J.V., Adriaensen, K. (2013) Zinc export results in adaptive zinc tolerance in
363 the ectomycorrhizal basidiomycete *Suillus bovinus*. Metallomics 5: 1225-1233
364 Sácký, J., Leonhardt, T., Kotrba P. (2016) Functional analysis of two genes coding for
365 distinct cation diffusion facilitators of the ectomycorrhizal Zn-accumulating fungus
366 Russula atropurpurea. Biometals 29:349–363.
367 Sekler, I., Sensi, S.L., Herschfinkel, M., Silverman, W.F. (2007) Mechanism and regulation
368 of cellular zinc transport. Mol Med 13(7-8): 337-343.

Simm, C., Lahner, B., Salt, D., LeFurgey, A., Ingram, P., Yandell, B., Eide, D.J. (2007) *Saccharomyces cerevisiae* vacuole in zinc storage and intracellular zinc distribution. Eukaryot Cell 6: 1166-1177.

Smith S.E., Read D.J. (2008) Mycorrhizal symbiosis (third edition). Academic Press.

Yin, J., Li, G., Ren, X., Herrler, G. (2007) Select what you need: a comparative evaluation of the advantages and limitations of frequently used expression systems for foreign genes. J Biotechnol 127: 335-347.

Supplementary Table 1. Degenerative primers used in the genome walking protocol.

name	sequence
DG1aS	GTNGCNGAYAGYTTYCAYATGCT
DG1bS	ATYGCNGAYTCATTYCAYATG
DG2aS	CAMCGWGCRGARATTCTNGCNGC
DG2bS	AAMGNGCRGARATTTTRGGTGCT
DG3aS	CTTGCSCTNTGYNTCTCNAT
DG3bS	ATTGCCYTNTGYNTSTYNATT
DG4aAS	AGNASASCAYGCATRTTCAT
DG4bAS	AASACACCATGCATATATTYAA
DG5aAS	CCNACRTTNCCNAGRGCRTC
DG5bAS	RCCRATRTTRCCNAGAGCATC
DG6aAS	TCNAARTARTAYTTCCARCTCCA
DG6bAS	RTARTANYKCCAAGAATAKTCRGT

Supplementary Table 2. Gene specific primers used in the different protocols.

name	sequence	target	protocol
ZnT1L	GGCATCACGAAACCATGACTTCAT	ZnT1	walking/RACE/gene expression
ZnT1R	GGTACTCGGGTTGAATAGTACTAGAATGT	ZnT1	walking/RACE/gene expression
ZnT1a	TCGGAGGAGTCTTATGGTCG	ZnT1	walking/RACE
ZnT1b	TGCGGGGGCGTATAATGAGA	ZnT1	walking
ZnT1c	CCTGGAGTAAAGAAGCGCTCT	ZnT1	walking
ZnT1d	CCTGCAATGAGCTCAATGAAGAAGAAGAA	ZnT1	walking
ZnT1Ra	ACATTCTAGTACTATTCAACCCGAGTACC	ZnT1	walking/RACE
ZnT2L	CGACGGTAAGGTGGAAATAAAC	ZnT2	walking/RACE/gene expression
ZnT2R	TGGTGAGCCAGATGACAAGA	ZnT2	walking/RACE/gene expression
ZnT2a	CCATGCGAATGAGAGTGACCA	ZnT2	walking
ZnT2b	CCAGCCGTAGGAGTAACGA	ZnT2	walking
ZnT2c	GATGCGAGCTGAACGAGATAA	ZnT2	walking/RACE
ZnT2d	CGTCATTACATCTTCCAGAACATTCCAT	ZnT2	walking

Figure 1. Labile Zn pool, marked with FluoZin 3, in *S. luteus*. (a-c) Overview of peripheral hyphae of the mycelium; (d-f) detailed view of hyphae showing vacuoles. (a,d) Differential interference contrast image, (b,e) green fluorescence of labile Zn bound to FluoZin3, (c,f) merged image showing fluorescence in vacuoles. Scale bars: (a-c) 10 µm; (d-f) 5 µm.

Figure 2. Alignment of SlZnT1 and SlZnT2 encoded proteins. Residues are Rasmol coloured. The six transmembrane domains predicted by topology prediction program TMHMM are indicated by arrows; the histidine rich motifs $(HX)_n$ between transmembrane helix IV and V are indicated by braces. The Zn specific HXXXD domains are framed by a dotted box.

Figure 3. Neighbour-joining (NJ) tree of the Cation Diffusion Facilitator (CDF) family proteins from selected fungi. Sequences were aligned by the MAFFT algorithm. Bootstrap values (1000 replicates) are indicated and branch lengths are proportional to phylogenetic distances. Localization and substrate (metal) are indicated for functionally characterized proteins. Mn and Fe clusters are collapsed. *S. luteus* sequences are framed, SlZnT1 and SlZnT2 are indicated by an arrow. V = vacuole; ER = endoplasmic reticulum, G = Golgi apparatus.

Figure 4. Functional complementation of the Zn sensitive yeast mutant Δzrc1. Cultures of wild type and mutant yeast were tenfold serial diluted and spotted on control and Zn-supplemented SD medium. The wild type strain was transformed with the empty vector, the mutant strain with either the empty vector or the vector containing *SlZnT1* or *SlZnT2*. The experiment was carried out twice for three independent clones and pictures were taken after 4 days of growth.

Figure 5. Localisation of SlZnT1:EGFP (a-d) and SlZnT2:EGFP (e-h) fusion proteins in yeast. (a,e) bright field image, (b,f) EGFP fusion protein, (c,g) FM4-64 vacuolar membrane

staining, (d, h) merged images. SlZnT1:GFP and FM4-64 tonoplast staining co-localize and SlZnT2:GFP is detected inside the vacuole.

Figure 6. Relative gene expression level of (a) SlZnT1 and (b) SlZnT2 in *S. luteus* mycelium after 48h exposure to different concentrations of Zn as measured by qPCR. Data are the average +/- SE of seven biological replicates. Both genes were constitutively expressed, no significant differences as compared to the control were detected.

Supplemental Figure S1. Gene model for the two newly identified *S. luteus* transporters, (a) *SlZnT1* and (b) *SlZnT2*. Untranslated regions (UTRs) are coloured green, exons red and introns are represented by a line. Length (amount of nucleic acids) of each individual part is indicated above (UTR and exon) or beneath (intron) the corresponding region.

Supplemental Figure S2. Evolution of fungal CDF transporters of the zrc1/cot1 cluster. Reconciled tree of the zrc1/cot1 cluster of CDF transporters using a maximum likelihood ITS phylogeny of selected fungal species supporting five independent gene duplication events (indicated in red). Seven gene loss events were predicted (represented in grey). *SlZnT1* and *SlZnT2* originate from a duplication event (indicated by an arrow) in the common ancestor of Suillineae and Coniophora/Serpula clade.

Supplemental Figure S3. Neighbour-joining (NJ) tree of the Cation Diffusion Facilitator (CDF) family proteins from selected fungi. Sequences were aligned by the MAFFT algorithm. Bootstrap values (1000 replicates) are indicated and branch lengths are proportional to phylogenetic distances. Localization and substrate (metal) are indicated for functionally characterized proteins. *S. luteus* sequences are framed. Zn clusters are collapsed. V = vacuole; ER = endoplasmic reticulum, G = Golgi apparatus.

Supplemental Figure S4. Heterologous expression of *SlZnT1* and *SlZnT2* in yeast mutants. Cultures of wild type and mutant yeast were tenfold serial diluted and spotted on control and metal-supplemented SD medium. The wild type strain was transformed with the

empty vector, the mutant strains with either the empty vector or the vector containing *SlZnT1* or *SlZnT2*. (a) A Co sensitive mutant Δcot1, (b) a Cd sensitive mutant Δycf and (c) a Mn sensitive strain Δpmr1 were used. The experiment was carried out twice for three independent clones and pictures were taken after 4 days of growth.

Supplemental Figure S5. PCR-product separated on gel-red stained 0.8% agarose gel. (a) PCR using *SlZnT2* targeting primers was run on cDNA samples of transformed yeast cells and plasmid DNA (positive control). SlZnT2 transcript was detected in Δzrc1 yeast cells transformed with SlZnT2 containing plasmid but not in cells transformed with the empty vector (EV). (b) A PCR using primers targeting the plasmid was performed to control for plasmid contamination of RNA samples. A PCR-product was detected for the plasmid DNA sample only. The PCRs were carried out for three independent clones.

Supplemental Figure S6. Zn concentration in transformed yeast cells in control conditions or after exposure to Zn. The wild type strain was transformed with the empty vector, the mutant strain with either the empty vector or the vector containing *SlZnT1* or *SlZnT2*. Data are the average +/- SE of three biological replicates, significant differences ($p < 0.01$; two-way ANOVA followed by Student-Newman-Keuls) are indicated by different letters.

Supplemental Figure S7. Fe and Mn concentration in transformed yeast cells in control conditions or after exposure to Zn. The wild type strain was transformed with the empty vector, the mutant strain with either the empty vector or the vector containing *SlZnT1* or *SlZnT2*. Data are the average +/- SE of three biological replicates, significant differences ($p < 0.01$; two-way ANOVA followed by Student-Newman-Keuls) are indicated by different letters.

Experimental procedures

Fungal material and growth conditions

The isolate UH-Slu-P4 from a *Suillus luteus* basidiocarp collected in a pine plantation in Paal, Belgium was used. Mycelium was cultured for one week on cellophane-covered solid Fries medium (28 mM glucose, 5.4 mM ammonium tartrate, 1.5 mM KH_2PO_4, 0.4 mM $MgSO_4 \cdot 7H_2O$, 5 µM $CuSO_4 \cdot 5H_2O$, 20 µM $ZnSO_4 \cdot 7H_2O$, 0.1 µM biotin, 0.5 µM pyridoxine, 0.3 µM riboflavin, 0.8 µM nicotinamide, 0.7 µM p-aminobenzoic acid, 0.3 µM thiamine, 0.2 µM Ca-pantothenate and 0.8% agar; pH-adjusted to 4.8) as described by Colpaert *et al.* (2004). Fungal colonies were used immediately in DNA and RNA extraction protocols or to prepare liquid cultures according to Ruytinx *et al.* (2016). After one week, 1 g of spherical mycelia grown in liquid culture was transferred to a petri dish containing 30 ml modified liquid Fries medium with a concentration of 0, 20, 200 or 1000 µM Zn and incubated shaking for 48h at 23°C. Zinc exposure was performed in triplicate. Spherical mycelia (200 mg) were stored at -70°C for gene expression analyses or used directly for staining of labile Zn pool.

Localization of labile Zn pool in *S. luteus*

Spherical mycelia obtained from liquid cultures exposed to different concentrations of Zn (20, 200, 1000 µM) were mixed in fresh medium of the same composition and grown for two additional days. Five mg FW mycelium was transferred to a 2 ml eppendorf tube with 1.5 ml TBS (Tris Buffered Saline: 137 mM NaCl, 3 mM KCl, 25 mM Tris; pH 7) containing 5µM FluoZin3. Following an incubation of 30 min (shaking), mycelia were washed twice in TBS for 5 min. FluoZin3 fluorescence was visualized with a Zeiss LSM 510 META laser scanning confocal microscope, using a Zeiss 40x NA1.3 oil immersion objective. The 488 nm excitation line of the laser and a BP 500-550 nm emission filter were used. Image processing was carried out with ImageJ (NIH, Bethesda, MD, USA) software.

DNA extraction and genome walking

Fungal material (100 mg fresh weight) was thoroughly ground in liquid nitrogen using a mortar and pestle. DNA was extracted from the grounded tissue using the DNeasy Plant mini kit (Qiagen). Concentration of the DNA was determined on a NanoDrop ND-1000 spectrophotometer and agarose gel analysis was used to control integrity. High quality DNA was used in a genome walking protocol (Genome Walker kit, Clontech). Briefly, DNA was digested by blunt end restriction enzymes, fragments were adaptor ligated and PCR was performed using an adaptor primer and a gene specific primer. Degenerative primers (Supplementary table 1) were designed based on 6 conservative domains of functionally characterized fungal Zn-CDF transporters. Fifty µl reactions containing 10x Advantage 2 PCR Buffer, 0.2 mM dNTP mix, 0.2 µM adaptor and gene specific primer, 50x Advantage 2 Polymerase Mix (Clonetech) and 1µl fungal DNA were performed using touchdown cycling conditions (7 cycles of 25s at 94°C, 3 min at 70°C; 32 cycles of 25s at 94°C, 3 min at 67°C and 1 cycle of 7 min at 67°C). Amplicons were visualised on a 1.5% agarose/gelred (Molecular Probes) gel, excised and resolved using the QIAquick Gel Extraction kit (Qiagen). Finally, PCR products were cloned into the pCR4-TOPO vector (Invitrogen) and sequenced. Sequences were assembled using the Staden Package v1.6.0. (www.Staden.SourceForge.net). New gene specific primers (Supplementary table 2) were designed and the protocol was repeated until the whole gene sequence was obtained.

RNA isolation, cDNA synthesis and rapid amplification of cDNA ends

Total RNA was extracted from in liquid nitrogen ground fungal colonies (200 mg) using the RNeasy Plant Mini Kit (Qiagen). RNA quality was assessed using the Agilent-2100 Bioanalyser and RNA 6000 NanoChips (Agilent Technologies). Poly(A)$^+$ RNA was isolated from 250 µg samples of total RNA using Oligotex columns (Qiagen). One µg poly(A) $^+$ RNA was converted into double stranded cDNA and adaptor ligated using the Marathon cDNA Amplification Kit

(Clontech) following the manufacturer's instructions. cDNA was diluted 50x in Tricine-EDTA buffer. RACE PCR was performed in 50 µl reactions containing 10x Advantage 2 PCR Buffer, 0.2 mM dNTP mix, 0.2 µM adaptor and gene specific primer (Supplementary table 2), 50x Advantage 2 Polymerase Mix (Clontech) and 5 µl diluted cDNA. PCR-products were visualised on a 1.5% agarose/gelred (Molecular Probes) gel and excised from the gel. After isolation and clean up of the PCR-products (QIAquick Gel Extraction kit; Qiagen), they were cloned into the pCR4-TOPO vector (Invitrogen) and sequenced. Sequences were assembled and aligned to the gDNA sequences to identify gene structure. *In silico* translations were performed and transmembrane domains predicted by TMHMM. The identified protein sequences were called ZnT1 and ZnT2. All bio-informatic analyses were performed using CLC Main workbench 6.7 and plug-ins unless stated otherwise.

Phylogenetic tree construction and reconciliation

BLASTx against NCBI nr protein sequences and JGI Agaricomycotina gene catalog proteins (using MycoCosm; Grigoriev *et al.*, 2012) was performed using the identified proteins and the CDF-family domain as a query. CDF-family proteins of *S. luteus* and selected Ascomycota and Basidiomycota species were inventoried using the following criteria: protein length between 350-700 amino acids, minimum 5 predicted transmembrane domains, presence of a CDF conserved domain or signature sequence (Montanini et al., 2007). The inventoried protein sequences were aligned together with previously functionally characterized fungal CDF transporters. This alignment was used for phylogenetic tree construction using the neighbour-joining (NJ) method. Bootstrap tests were conducted using 1000 replicates and branch lengths are proportional to phylogenetic distance. A species tree was build using ITS-sequences retrieved from the UNITE database. Phylogenetic trees were built in MEGA v6.06; NOTUNG v2.8.1.7 was used to reconcile both phylogenies.

Cloning

One µg total RNA was used in a Quantiscript Reverse Transcription reaction (Qiagen), which includes a genomic DNA elimination step and makes use of random hexamer priming. Specific primers were designed to amplify full-length coding sequences of *SlZnT1* (left: attcactcaacactcagcactcg; right: aacgcctgagacgggcgga) and *SlZnT2* (left: gtgccaaccacaatggcat; right: tagtatcacagtggtcgg). PCR reactions were performed in a total volume of 25 µl, containing 10x High Fidelity PCR buffer, 0.2 mM dNTP-mixture, 2 mM MgSO4, 0.2 µM specific forward and reverse primer, 1 µl cDNA and 0.5 U Platinum Taq High Fidelity DNA polymerase (Invitrogen) using general cycling conditions (2 min at 95°C, 35 cycles of 30s at 95°C, 30s at 60°C, 1 min at 68°C, 1 cycle of 2 min at 68°C). Amplicons were purified using QIAquick PCR purification Kit (Qiagen) according to manufactures instructions. Purified PCR-products were cloned into the gateway entry vector pCR8/GW/TOPO (Invitrogen) and subsequentially transferred by LR-clonase (Invitrogen) to pYES-DEST52 (Invitrogen), pAG306GAL-ccdB-EGFP or pAG306GAL-EGFP-ccdB (Alberti *et al.*, 2007) for complementation, Zn content analysis and localisation by GFP fluorescence in yeast. Finally, the insert was sequenced in both directions to assure correct fusion.

Yeast mutant complementation

The yeast strains used for heterologous expression of *SlZnT1* and *SlZnT2* are BY4741 (MAT a; his3Δ1; leu2Δ; met15Δ0; ura3Δ0), Δzrc1 (BY4741; MAT a; his3Δ1; leu2Δ; met15Δ0; ura3Δ0; YMR243c::kanMX4), Δcot1 (BY4741; Mat a; his3Δ1; leu2Δ; met15Δ0; ura3Δ0; YOR316c::kanMX4), Δycf1 (BY4741; Mat a; his3Δ1; leu2Δ; met15Δ0; ura3Δ0; YDR135c::kanMX4) and Δpmr1 (BY4741; Mat a; his3Δ1; leu2Δ; met15Δ0; ura3Δ0; YGL167c::kanMX4) obtained from Euroscarf (http: www.uni-frankfurt.de/fb15/mikro/euroscarf). Yeast cells were transformed according to the LiAc/PEG

method described by Gietz & Woods (2002). After transformation, cells were grown at 30°C in synthetic defined (SD) medium without amino acids, containing 2% (w/v) glucose or galactose (induction medium), supplemented with yeast synthetic dropout without uracil, (pH5.3). Positive colonies were PCR tested to confirm transformation. For metal tolerance assays, yeast was grown on induction medium to an OD_{600nm} of one to perform tenfold dilution series. The drop assays were performed for three independent clones on control SD plates (2% w/v galactose) and SD plates supplemented with 8 mM Zn; 30 µM Cd; 1 mM Co or 1 mM Mn. RNA was extracted from colonies growing on control plates and converted in cDNA to verify transcription of the transgene by PCR.

Localisation by confocal imaging

Yeast cells were transformed, expression was induced by galactose and functionality of the gene product was tested as described previously (see yeast mutant complementation). Cells were grown to an OD_{600nm} of one, vacuolar membranes were selectively stained with the red fluorescence probe FM4-64 (Molecular Probes, Invitrogen) following Vida & Emr (1995). A 3 µl droplet of yeast cells was analyzed at 20°C with a Zeiss LSM 510 META laser scanning confocal microscope, using a Zeiss 63x NA1.4 oil immersion objective and 10x scanning zoom at 512x512 pixel resolution (image size: 8 bit, 14,62 µm²). For EGFP fluorescence analysis we used the 488 nm excitation line of the laser and a BP 500-550 nm emission filter. For FM4-64 fluorescence analysis we used the 488 nm excitation line of the laser and a LP 560 nm emission filter. Image processing was carried out with ImageJ (NIH, Bethesda, MD, USA) software.

Zn content analysis of transformed yeast

Yeast cells were transformed and expression was induced as described in "yeast mutant complementation". Wild type yeast containing the empty vector, Δzrc1 yeast containing the empty vector and Δzrc1 yeast containing the *SlZnT1* or *SlZnT2* cDNA were grown in liquid SD

medium containing galactose and supplemented with different concentrations of Zn (0 µM or 500 µM). Zn treatments were performed for three independent clones. Yeast cells were harvested when OD_{600nm} of the cultures equalled one. Cells were washed three times with 20 mM $PbNO_3$ and milli-Q water. After drying, cells were destructed in concentrated acid (HNO_3/HCl) and Zn content was determined by inductively coupled plasma optical emission spectrometry (ICP-OES).

Gene expression analysis

Total RNA extraction and cDNA synthesis occurred as described before. Real-time PCR was carried out in 10 µl reactions containing fast SYBR Green Master Mix (Applied Biosystems), 300 nM gene-specific forward (ZnT1L or ZnT2L; supplementary table 2) and reverse primer (ZnT1R or ZnT2R; supplementary table 2) and 2.5µl diluted cDNA (fivefold dilution in 1/10 Tris-EDTA buffer). An ABI PRISM 7500 sequence detection system (Applied Biosystems) and fast cycling conditions (20s at 95°C, 40 cycles of 3s at 95°C and 30s at 60°C) were used. After cycling, a dissociation stage was added to assure specificity of amplification. Data were expressed relative to the sample with the highest expression ($2^{-(Ct-Ctmax)}$) and normalised against four reference genes. GR975621, AM085297, AM085168 and TUB1 were used as reference genes according to Ruytinx *et al.* (2016). The normalisation factor for each sample was calculated as the geometric mean of the relative expression of the four reference genes. The significance of differences in expression level was examined by 2-way ANOVA and Tukey post-test.

References

Alberti, S., Gitler, A.D., Lindquist, S. (2007) A suite of gateway cloning vectors for high-throughput genetic analysis in *Saccharomyces cerevisiae*. Yeast 24(10): 913-919.

Colpaert, J.V., Muller, L.A.H., Lambaerts, M., Adriaensen, K., Vangronsveld, J. (2004) Evolutionary adaptation to Zn toxicity in populations of Suilloid fungi. New Phytol 162: 546-559.

Gietz, D.R., Woods, R.A. (2002) Transformation of yeast by lithium acetate/single-stranded carrier DNA/polyethylene glycol method. Method Enzymol 350: 87-96.

Grigoriev, I., Nordberg, H., Shabalov, I., Aerts, A., Cantor, M., Goodstein, D., Kuo, A., Minovitsky, S., Nikitin, R., Ohm, R. *et al.* 2012. The genome portal of the department of energy joint genome institute. Nucleic Acids Res 40(D1): D26-D32.

Montanini, B., Blaudez, D., Jeandroz, S., Sanders, D., Chalot, M. (2007) Phylogenetic and functional analysis of the cation diffusion facilitator (CDF) family: improved signature and prediction of substrate specificity. BMC Genomic 8: 107-122.

Ruytinx, J., Remans, T., Colpaert, J.V. (2016) Gene expression studies in different genotypes of an ectomycorrhizal fungus require a high number of reliable reference genes. Peer J Preprints 4: e2125v1.

Vida, T.A., Emr, S.D. (1995) A new vital stain for visualizing vacuolar membrane dynamics and endocytosis in yeast. J Cell Biol 128(5): 779-792.

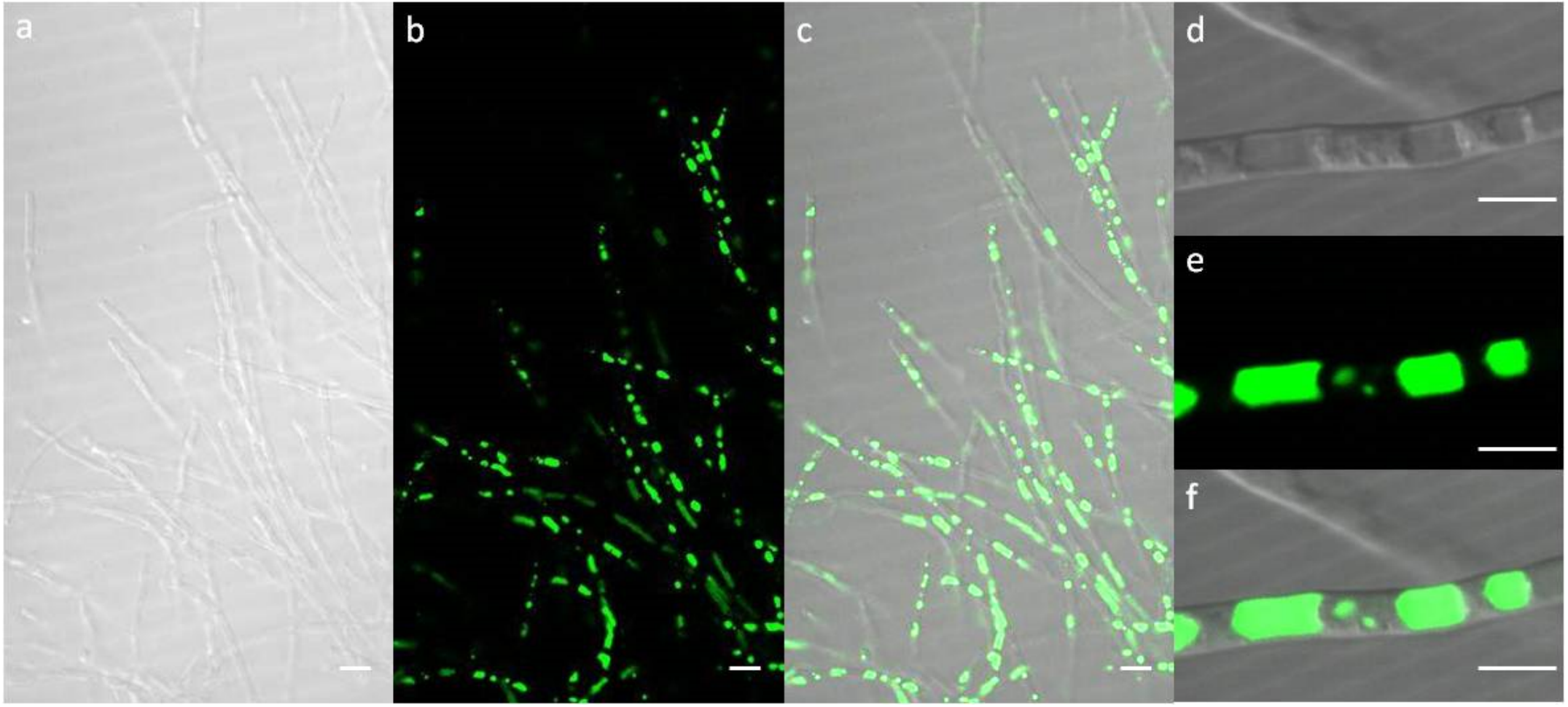
a
b
c
d
e
f

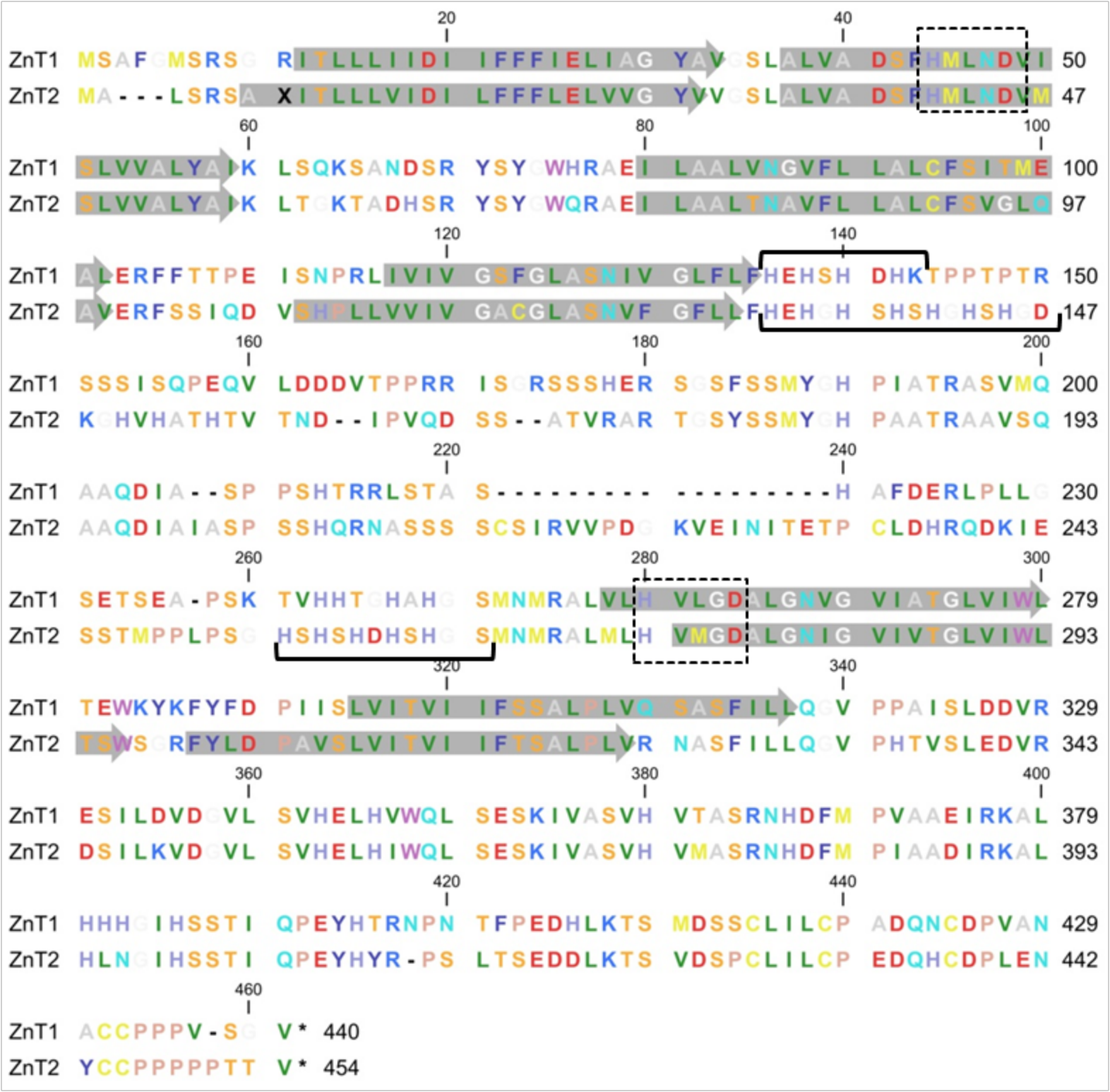
ZnT1 MSAFGMSRSG RITLLLIIDI IFFFIELIAG YAVGSLALVA DSFHMLNDVI 50
ZnT2 MA---LSRSA XITLLLVIDI LFFFLELVVG YVVGSLALVA DSFHMLNDVM 47
ZnT1 SLVVALYAIK LSQKSANDSR YSYGWHRAEI LAALVNGVFL LALCFSITME 100
ZnT2 SLVVALYAIK LTGKTADHSR YSYGWQRAEI LAALTNAVFL LALCFSVGLQ 97
ZnT1 ALERFFTTPE ISNPRLIVIV GSFGLASNIV GLFLFHEHSH DHKTPPTPTR 150
ZnT2 AVERFSSIQD VSHPLLVVIV GACGLASNVF GFLLFHEHGH SHSHGHSHGD 147
ZnT1 SSSISQPEQV LDDDVTPPRR ISGRSSSHER SGSFSSMYGH PIATRASVMQ 200
ZnT2 KGHVHATHTV TND--IPVQD SS--ATVRAR TGSYSSMYGH PAATRAAVSQ 193
ZnT1 AAQDIA--SP PSHTRRLSTA S--------- ---------H AFDERLPLLG 230
ZnT2 AAQDIAIASP SSHQRNASSS SCSIRVVPDG KVEINITETP CLDHRQDKIE 243
ZnT1 SETSEA-PSK TVHHTGHAHG SMNMRALVLH VLGDALGNVG VIATGLVIWL 279
ZnT2 SSTMPPLPSG HSHSHDHSHG SMNMRALMLH VMGDALGNIG VIVTGLVIWL 293
ZnT1 TEWKYKFYFD PIISLVITVI IFSSALPLVQ SASFILLQGV PPAISLDDVR 329
ZnT2 TSWSGRFYLD PAVSLVITVI IFTSALPLVR NASFILLQGV PHTVSLEDVR 343
ZnT1 ESILDVDGVL SVHELHVWQL SESKIVASVH VTASRNHDFM PVAAEIRKAL 379
ZnT2 DSILKVDGVL SVHELHIWQL SESKIVASVH VMASRNHDFM PIAADIRKAL 393
ZnT1 HHHGIHSSTI QPEYHTRNPN TFPEDHLKTS MDSSCLILCP ADQNCDPVAN 429
ZnT2 HLNGIHSSTI QPEYHYR-PS LTSEDDLKTS VDSPCLILCP EDQHCDPLEN 442
ZnT1 ACCPPPV-SG V* 440
ZnT2 YCCPPPPPTT V* 454

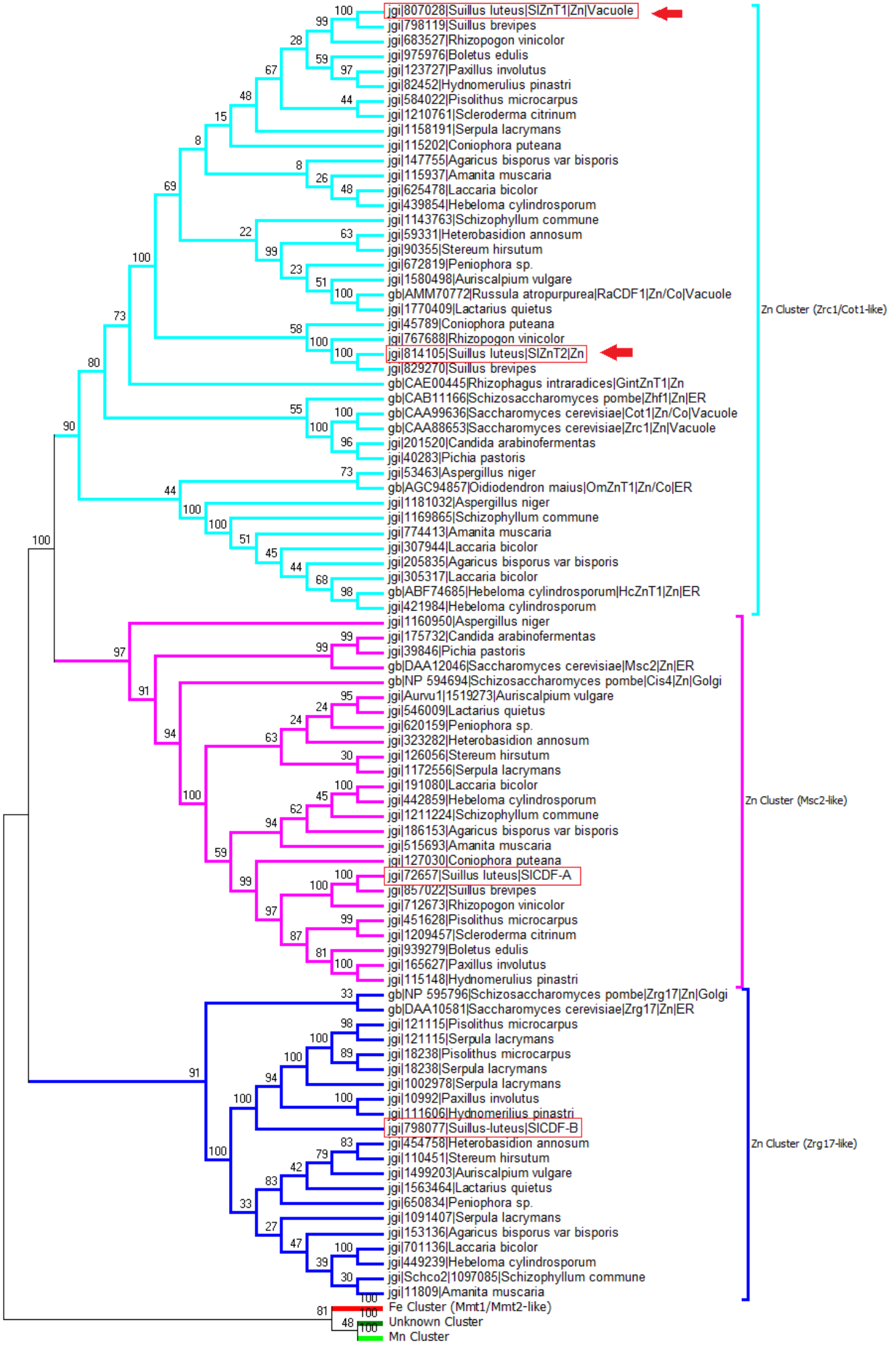
jgi|807028|Suillus luteus|SlZnT1|Zn|Vacuole
jgi|798119|Suillus brevipes
jgi|683527|Rhizopogon vinicolor
jgi|975976|Boletus edulis
jgi|123727|Paxillus involutus
jgi|82452|Hydnomerulius pinastri
jgi|584022|Pisolithus microcarpus
jgi|1210761|Scleroderma citrinum
jgi|1158191|Serpula lacrymans
jgi|115202|Coniophora puteana
jgi|147755|Agaricus bisporus var bisporis
jgi|115937|Amanita muscaria
jgi|625478|Laccaria bicolor
jgi|439854|Hebeloma cylindrosporum
jgi|1143763|Schizophyllum commune
jgi|59331|Heterobasidion annosum
jgi|90355|Stereum hirsutum
jgi|672819|Peniophora sp.
jgi|1580498|Auriscalpium vulgare
gb|AMM70772|Russula atropurpurea|RaCDF1|Zn/Co|Vacuole
jgi|1770409|Lactarius quietus
jgi|45789|Coniophora puteana
jgi|767688|Rhizopogon vinicolor
jgi|814105|Suillus luteus|SlZnT2|Zn
jgi|829270|Suillus brevipes
gb|CAE00445|Rhizophagus intraradices|GintZnT1|Zn
gb|CAB11166|Schizosaccharomyces pombe|Zhf1|Zn|ER
gb|CAA99636|Saccharomyces cerevisiae|Cot1|Zn/Co|Vacuole
gb|CAA88653|Saccharomyces cerevisiae|Zrc1|Zn|Vacuole
jgi|201520|Candida arabinofermentas
jgi|40283|Pichia pastoris
jgi|53463|Aspergillus niger
gb|AGC94857|Oidiodendron maius|OmZnT1|Zn/Co|ER
jgi|1181032|Aspergillus niger
jgi|1169865|Schizophyllum commune
jgi|774413|Amanita muscaria
jgi|307944|Laccaria bicolor
jgi|205835|Agaricus bisporus var bisporis
jgi|305317|Laccaria bicolor
gb|ABF74685|Hebeloma cylindrosporum|HcZnT1|Zn|ER
jgi|421984|Hebeloma cylindrosporum
Zn Cluster (Zrc1/Cot1-like)
jgi|1160950|Aspergillus niger
jgi|175732|Candida arabinofermentas
jgi|39846|Pichia pastoris
gb|DAA12046|Saccharomyces cerevisiae|Msc2|Zn|ER
gb|NP 594694|Schizosaccharomyces pombe|Cis4|Zn|Golgi
jgi|Aurvu1|1519273|Auriscalpium vulgare
jgi|546009|Lactarius quietus
jgi|620159|Peniophora sp.
jgi|323282|Heterobasidion annosum
jgi|126056|Stereum hirsutum
jgi|1172556|Serpula lacrymans
jgi|191080|Laccaria bicolor
jgi|442859|Hebeloma cylindrosporum
jgi|1211224|Schizophyllum commune
jgi|186153|Agaricus bisporus var bisporis
jgi|515693|Amanita muscaria
jgi|127030|Coniophora puteana
jgi|72657|Suillus luteus|SlCDF-A
jgi|857022|Suillus brevipes
jgi|712673|Rhizopogon vinicolor
jgi|451628|Pisolithus microcarpus
jgi|1209457|Scleroderma citrinum
jgi|939279|Boletus edulis
jgi|165627|Paxillus involutus
jgi|115148|Hydnomerulius pinastri
Zn Cluster (Msc2-like)
gb|NP 595796|Schizosaccharomyces pombe|Zrg17|Zn|Golgi
gb|DAA10581|Saccharomyces cerevisiae|Zrg17|Zn|ER
jgi|121115|Pisolithus microcarpus
jgi|121115|Serpula lacrymans
jgi|18238|Pisolithus microcarpus
jgi|18238|Serpula lacrymans
jgi|1002978|Serpula lacrymans
jgi|10992|Paxillus involutus
jgi|111606|Hydnomerilius pinastri
jgi|798077|Suillus-luteus|SlCDF-B
jgi|454758|Heterobasidion annosum
jgi|110451|Stereum hirsutum
jgi|1499203|Auriscalpium vulgare
jgi|1563464|Lactarius quietus
jgi|650834|Peniophora sp.
jgi|1091407|Serpula lacrymans
jgi|153136|Agaricus bisporus var bisporis
jgi|701136|Laccaria bicolor
jgi|449239|Hebeloma cylindrosporum
jgi|Schco2|1097085|Schizophyllum commune
jgi|11809|Amanita muscaria
Zn Cluster (Zrg17-like)
Fe Cluster (Mmt1/Mmt2-like)
Unknown Cluster
Mn Cluster

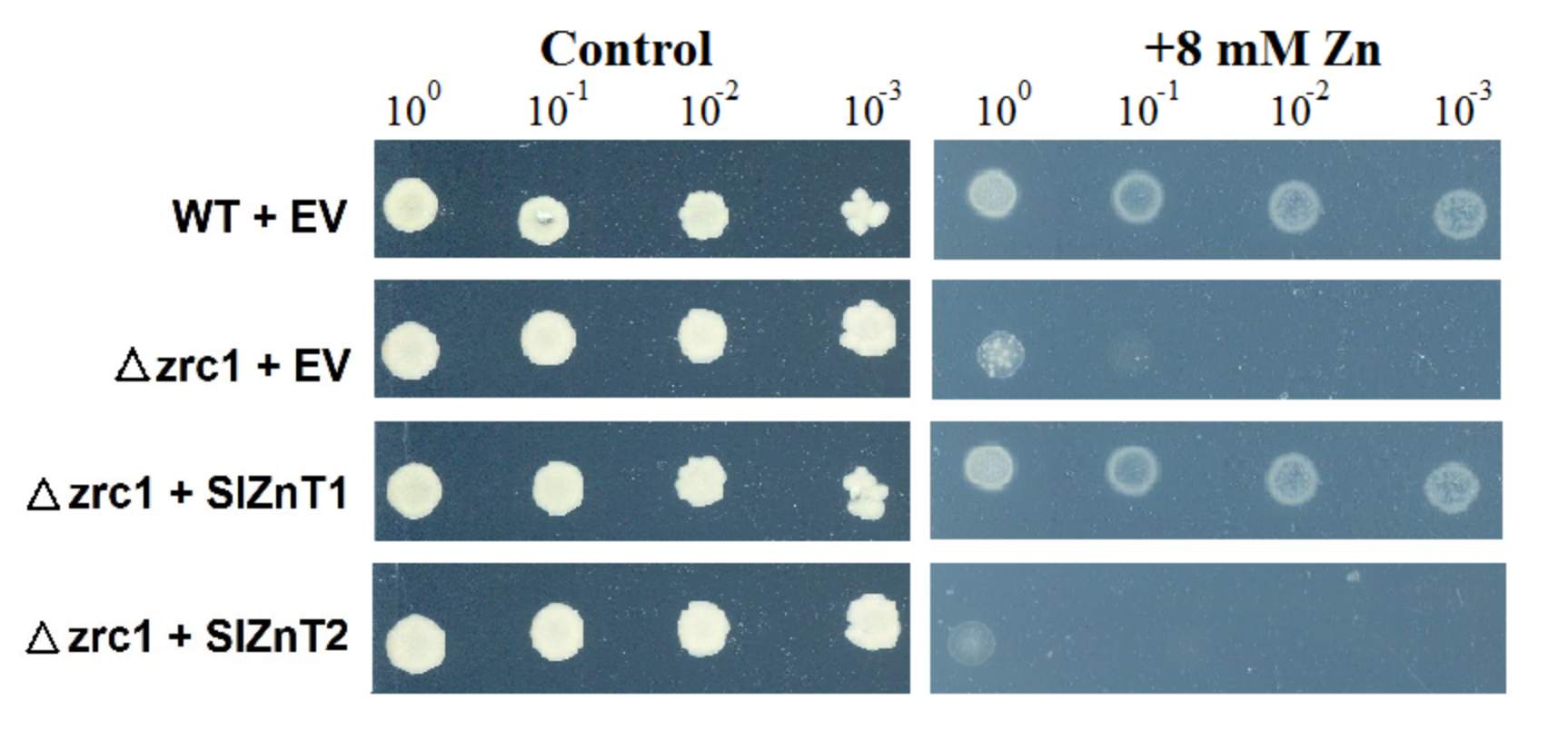
Control
+8 mM Zn
10^0
10^-1
10^-2
10^-3
10^0
10^-1
10^-2
10^-3
WT + EV
Δzrc1 + EV
Δzrc1 + SlZnT1
Δzrc1 + SlZnT2

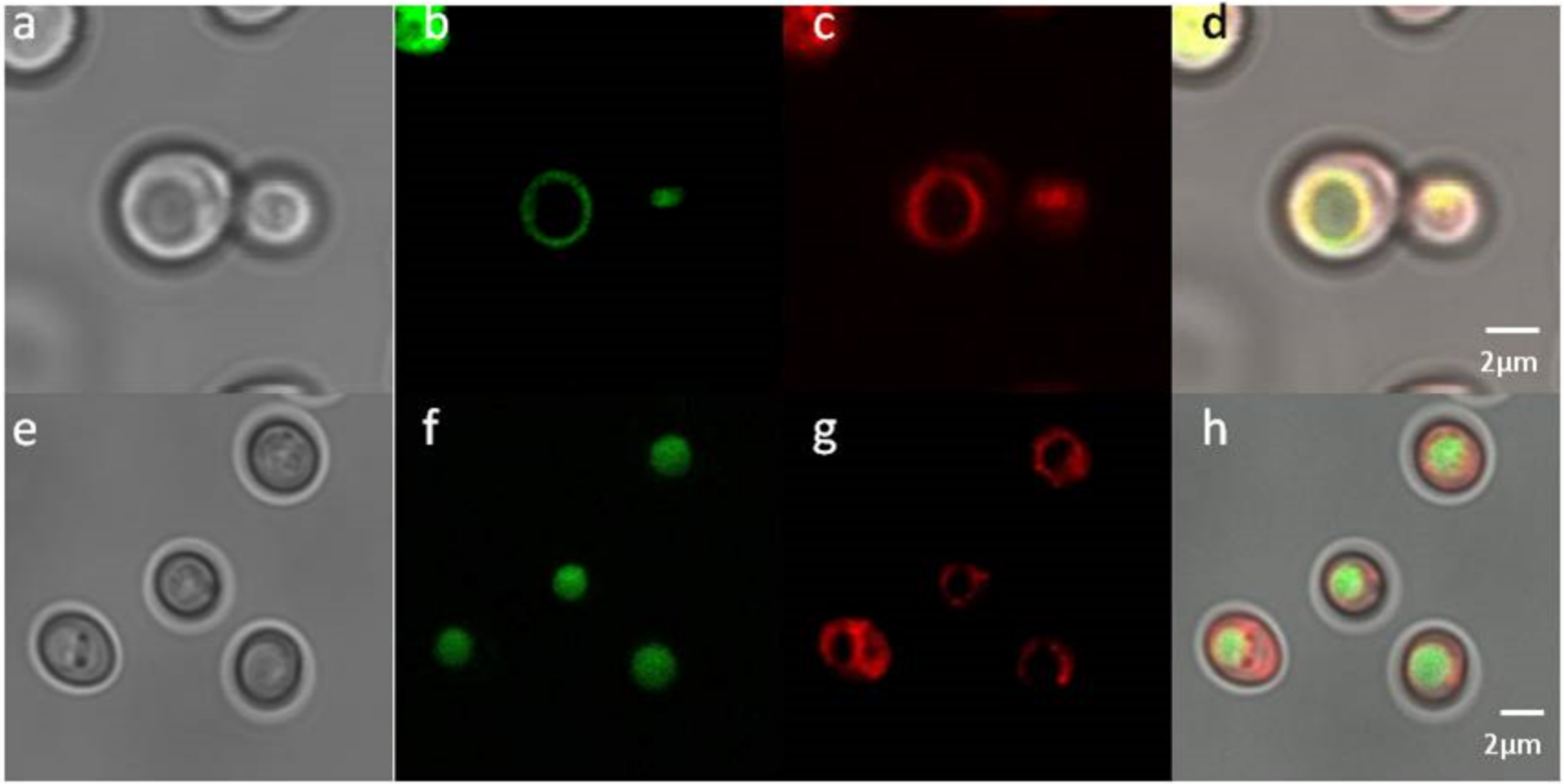
a
b
c
d
2µm
e
f
g
h
2µm

(a)

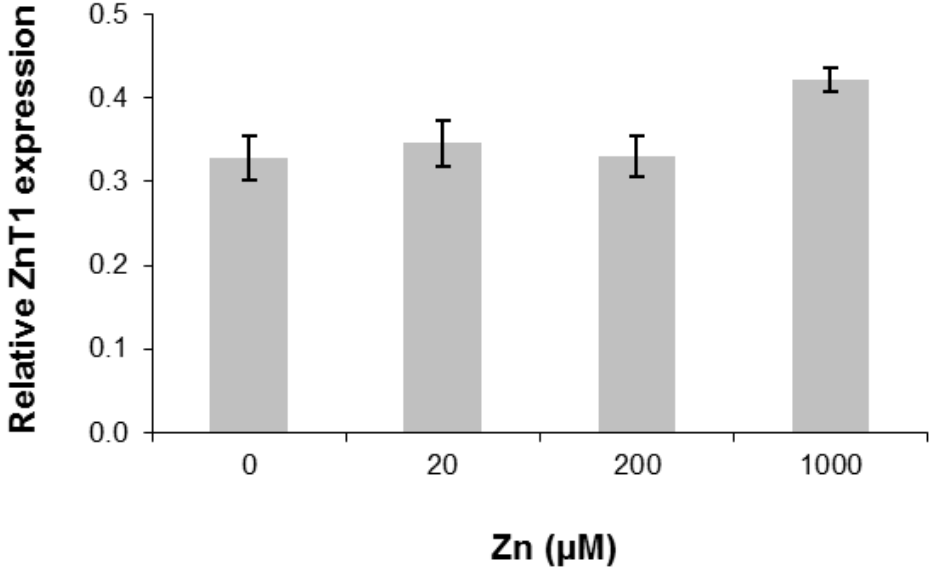
Relative ZnT1 expression
0.5
0.4
0.3
0.2
0.1
0.0
0
20
200
1000
Zn (μM)

(b)

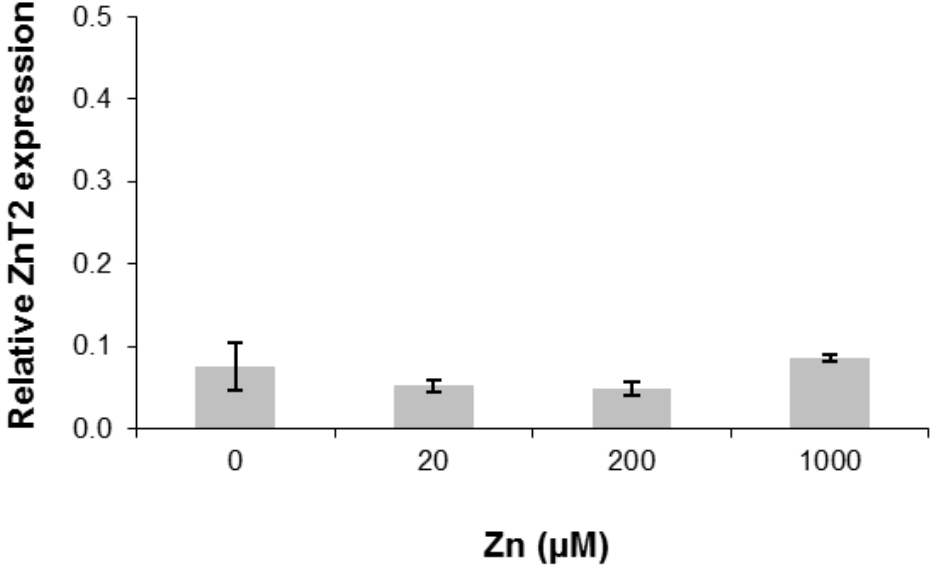
Relative ZnT2 expression
0.5
0.4
0.3
0.2
0.1
0.0
0
20
200
1000
Zn (μM)

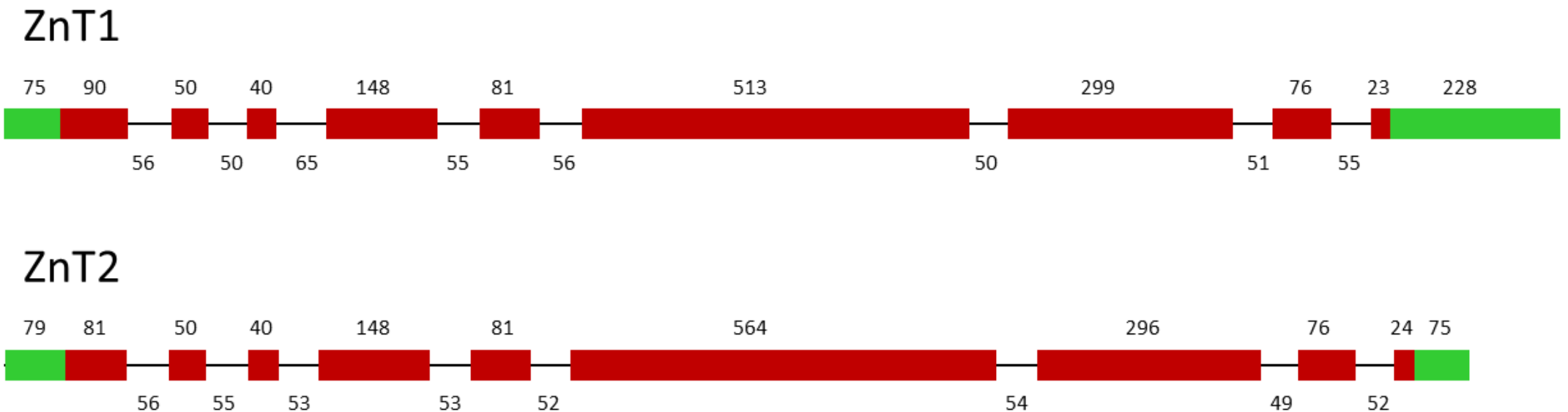
ZnT1
75
90
50
40
148
81
513
299
76
23
228
56
50
65
55
56
50
51
55
ZnT2
79
81
50
40
148
81
564
296
76
24
75
56
55
53
53
52
54
49
52

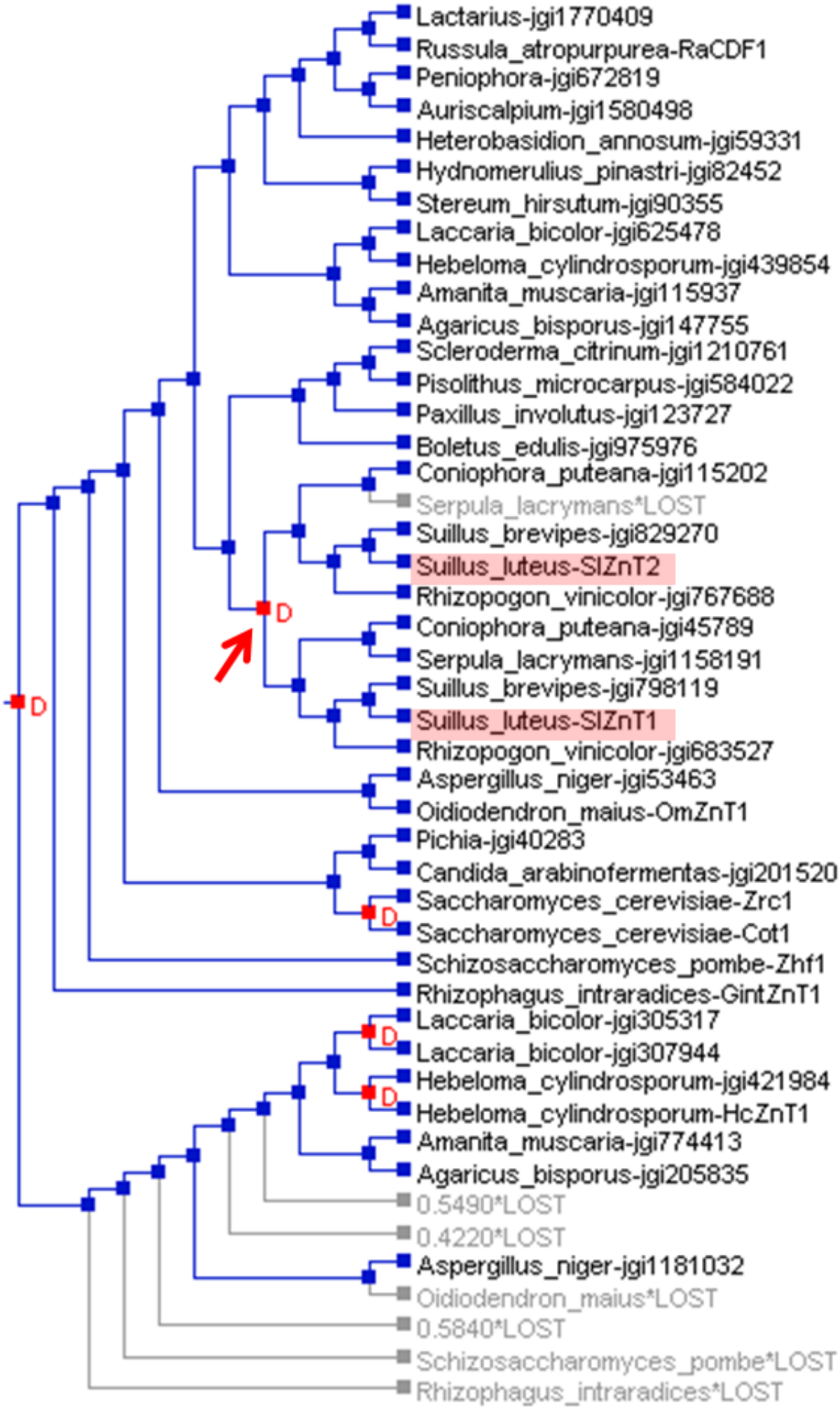
Lactarius-jgi1770409
Russula_atropurpurea-RaCDF1
Peniophora-jgi672819
Auriscalpium-jgi1580498
Heterobasidion_annosum-jgi59331
Hydnomerulius_pinastri-jgi82452
Stereum_hirsutum-jgi90355
Laccaria_bicolor-jgi625478
Hebeloma_cylindrosporum-jgi439854
Amanita_muscaria-jgi115937
Agaricus_bisporus-jgi147755
Scleroderma_citrinum-jgi1210761
Pisolithus_microcarpus-jgi584022
Paxillus_involutus-jgi123727
Boletus_edulis-jgi975976
Coniophora_puteana-jgi115202
Serpula_lacrymans*LOST
Suillus_brevipes-jgi829270
Suillus_luteus-SlZnT2
Rhizopogon_vinicolor-jgi767688
Coniophora_puteana-jgi45789
Serpula_lacrymans-jgi1158191
Suillus_brevipes-jgi798119
Suillus_luteus-SlZnT1
Rhizopogon_vinicolor-jgi683527
Aspergillus_niger-jgi53463
Oidiodendron_maius-OmZnT1
Pichia-jgi40283
Candida_arabinofermentas-jgi201520
Saccharomyces_cerevisiae-Zrc1
Saccharomyces_cerevisiae-Cot1
Schizosaccharomyces_pombe-Zhf1
Rhizophagus_intraradices-GintZnT1
Laccaria_bicolor-jgi305317
Laccaria_bicolor-jgi307944
Hebeloma_cylindrosporum-jgi421984
Hebeloma_cylindrosporum-HcZnT1
Amanita_muscaria-jgi774413
Agaricus_bisporus-jgi205835
0.5490*LOST
0.4220*LOST
Aspergillus_niger-jgi1181032
Oidiodendron_maius*LOST
0.5840*LOST
Schizosaccharomyces_pombe*LOST
Rhizophagus_intraradices*LOST
D
D
D
D
D

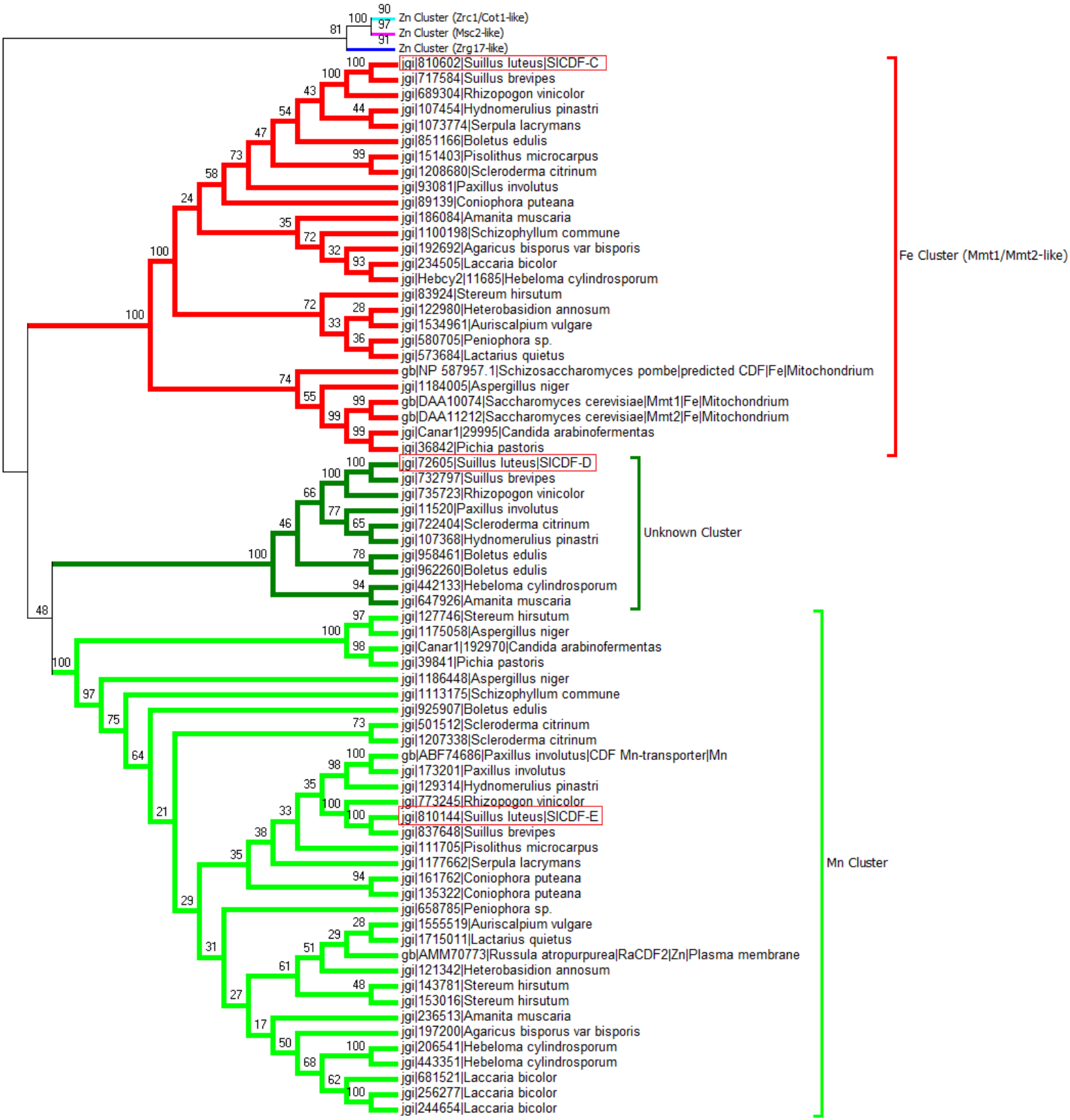
Zn Cluster (Zrc1/Cot1-like)
Zn Cluster (Msc2-like)
Zn Cluster (Zrg17-like)
jgi|810602|Suillus luteus|SlCDF-C
jgi|717584|Suillus brevipes
jgi|689304|Rhizopogon vinicolor
jgi|107454|Hydnomerulius pinastri
jgi|1073774|Serpula lacrymans
jgi|851166|Boletus edulis
jgi|151403|Pisolithus microcarpus
jgi|1208680|Scleroderma citrinum
jgi|93081|Paxillus involutus
jgi|89139|Coniophora puteana
jgi|186084|Amanita muscaria
jgi|1100198|Schizophyllum commune
jgi|192692|Agaricus bisporus var bisporis
jgi|234505|Laccaria bicolor
jgi|Hebcy2|11685|Hebeloma cylindrosporum
jgi|83924|Stereum hirsutum
jgi|122980|Heterobasidion annosum
jgi|1534961|Auriscalpium vulgare
jgi|580705|Peniophora sp.
jgi|573684|Lactarius quietus
gb|NP 587957.1|Schizosaccharomyces pombe|predicted CDF|Fe|Mitochondrium
jgi|1184005|Aspergillus niger
gb|DAA10074|Saccharomyces cerevisiae|Mmt1|Fe|Mitochondrium
gb|DAA11212|Saccharomyces cerevisiae|Mmt2|Fe|Mitochondrium
jgi|Canar1|29995|Candida arabinofermentas
jgi|36842|Pichia pastoris
Fe Cluster (Mmt1/Mmt2-like)
jgi|72605|Suillus luteus|SlCDF-D
jgi|732797|Suillus brevipes
jgi|735723|Rhizopogon vinicolor
jgi|11520|Paxillus involutus
jgi|722404|Scleroderma citrinum
jgi|107368|Hydnomerulius pinastri
jgi|958461|Boletus edulis
jgi|962260|Boletus edulis
jgi|442133|Hebeloma cylindrosporum
jgi|647926|Amanita muscaria
Unknown Cluster
jgi|127746|Stereum hirsutum
jgi|1175058|Aspergillus niger
jgi|Canar1|192970|Candida arabinofermentas
jgi|39841|Pichia pastoris
jgi|1186448|Aspergillus niger
jgi|1113175|Schizophyllum commune
jgi|925907|Boletus edulis
jgi|501512|Scleroderma citrinum
jgi|1207338|Scleroderma citrinum
gb|ABF74686|Paxillus involutus|CDF Mn-transporter|Mn
jgi|173201|Paxillus involutus
jgi|129314|Hydnomerulius pinastri
jgi|773245|Rhizopogon vinicolor
jgi|810144|Suillus luteus|SlCDF-E
jgi|837648|Suillus brevipes
jgi|111705|Pisolithus microcarpus
jgi|1177662|Serpula lacrymans
jgi|161762|Coniophora puteana
jgi|135322|Coniophora puteana
jgi|658785|Peniophora sp.
jgi|1555519|Auriscalpium vulgare
jgi|1715011|Lactarius quietus
gb|AMM70773|Russula atropurpurea|RaCDF2|Zn|Plasma membrane
jgi|121342|Heterobasidion annosum
jgi|143781|Stereum hirsutum
jgi|153016|Stereum hirsutum
jgi|236513|Amanita muscaria
jgi|197200|Agaricus bisporus var bisporis
jgi|206541|Hebeloma cylindrosporum
jgi|443351|Hebeloma cylindrosporum
jgi|681521|Laccaria bicolor
jgi|256277|Laccaria bicolor
jgi|244654|Laccaria bicolor
Mn Cluster

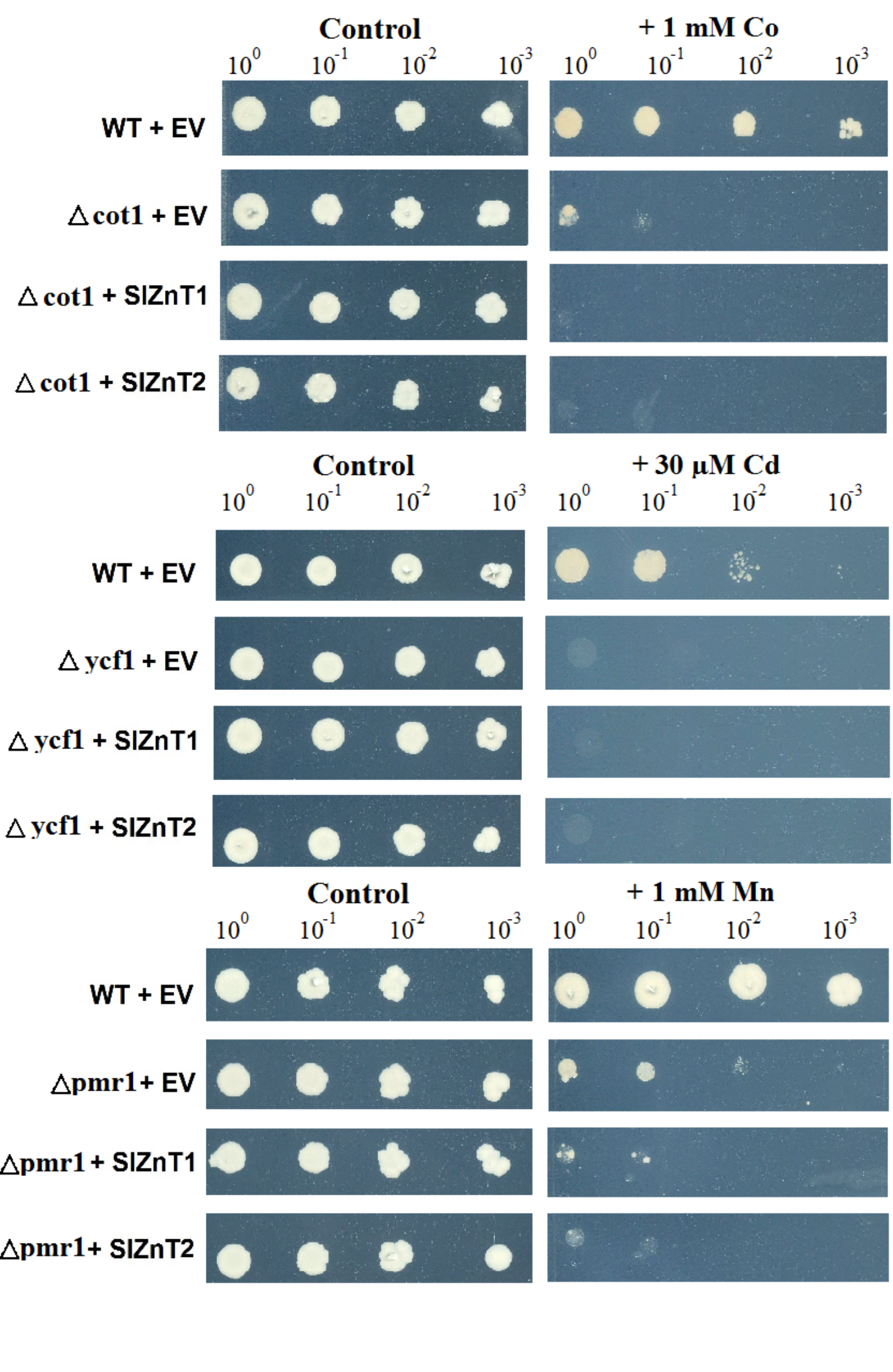
Control
+ 1 mM Co
10^0 10^-1 10^-2 10^-3
WT + EV
Δcot1 + EV
Δcot1 + SlZnT1
Δcot1 + SlZnT2
Control
+ 30 µM Cd
10^0 10^-1 10^-2 10^-3
WT + EV
Δycf1 + EV
Δycf1 + SlZnT1
Δycf1 + SlZnT2
Control
+ 1 mM Mn
10^0 10^-1 10^-2 10^-3
WT + EV
Δpmr1+ EV
Δpmr1 + SlZnT1
Δpmr1+ SlZnT2

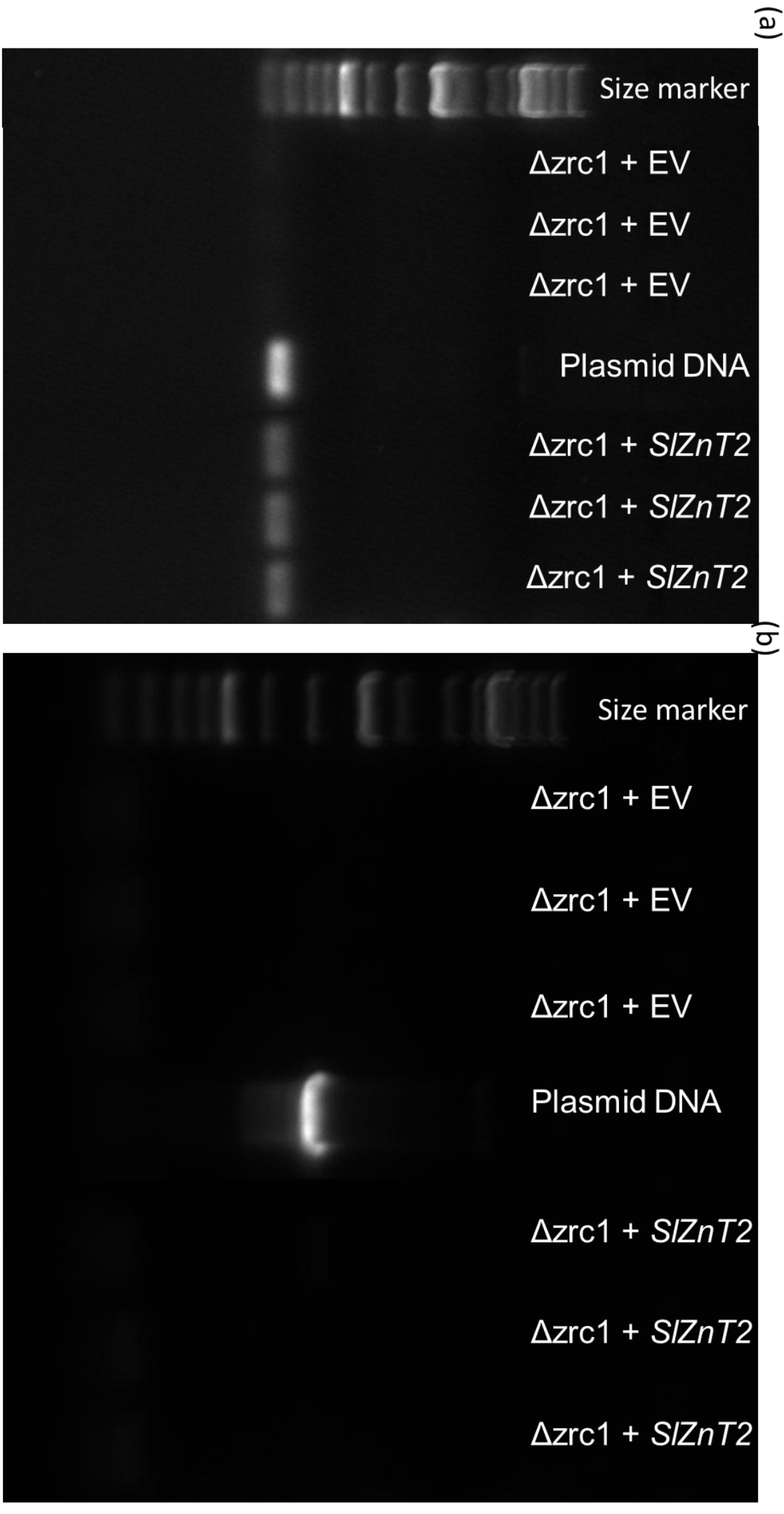
(a)
Size marker
Δzrc1 + EV
Δzrc1 + EV
Δzrc1 + EV
Plasmid DNA
Δzrc1 + SlZnT2
Δzrc1 + SlZnT2
Δzrc1 + SlZnT2
(b)
Size marker
Δzrc1 + EV
Δzrc1 + EV
Δzrc1 + EV
Plasmid DNA
Δzrc1 + SlZnT2
Δzrc1 + SlZnT2
Δzrc1 + SlZnT2

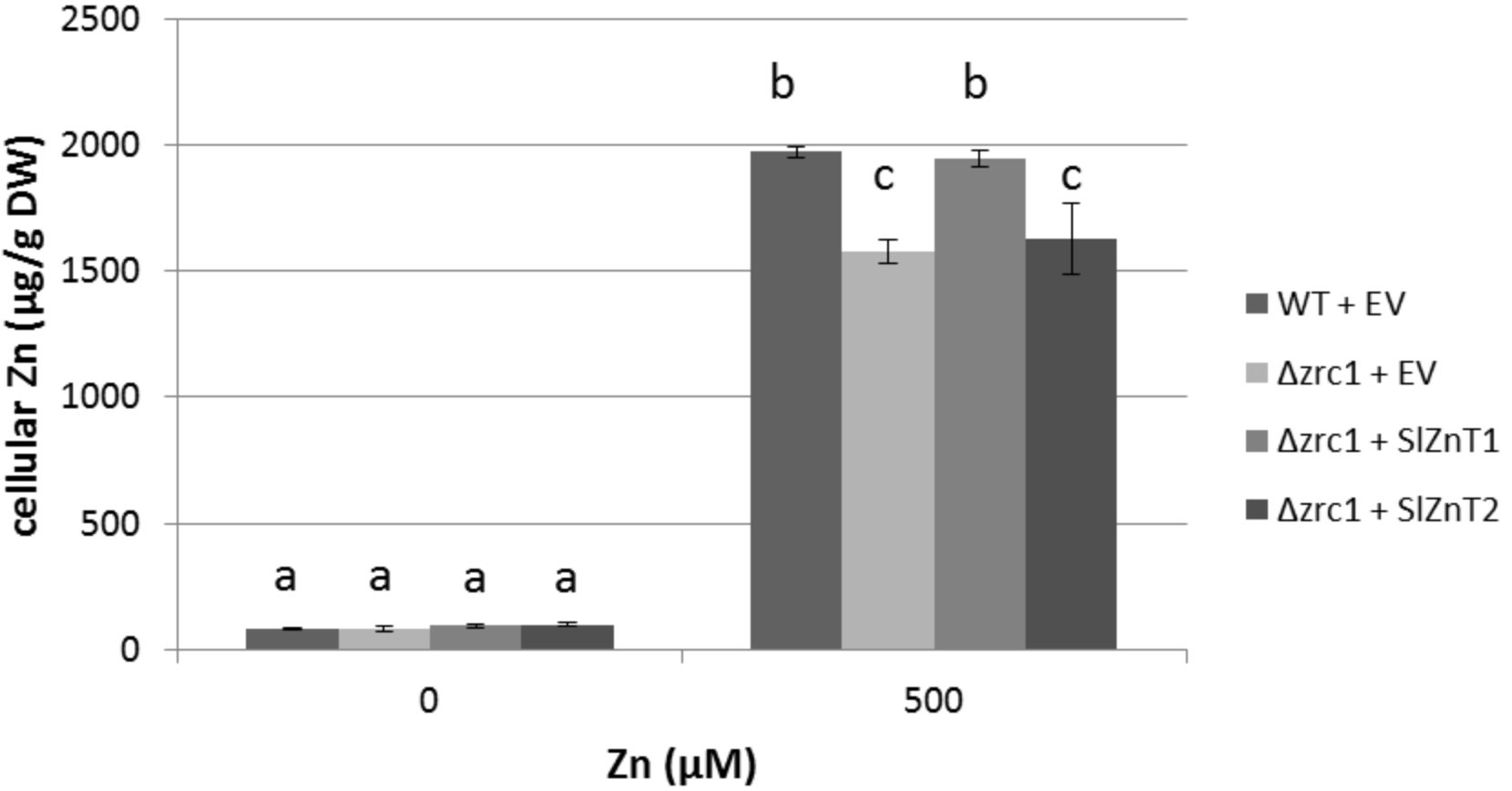
2500
2000
1500
1000
500
0
cellular Zn (µg/g DW)
a
a
a
a
b
c
b
c
0
500
Zn (µM)
WT + EV
Δzrc1 + EV
Δzrc1 + SlZnT1
Δzrc1 + SlZnT2

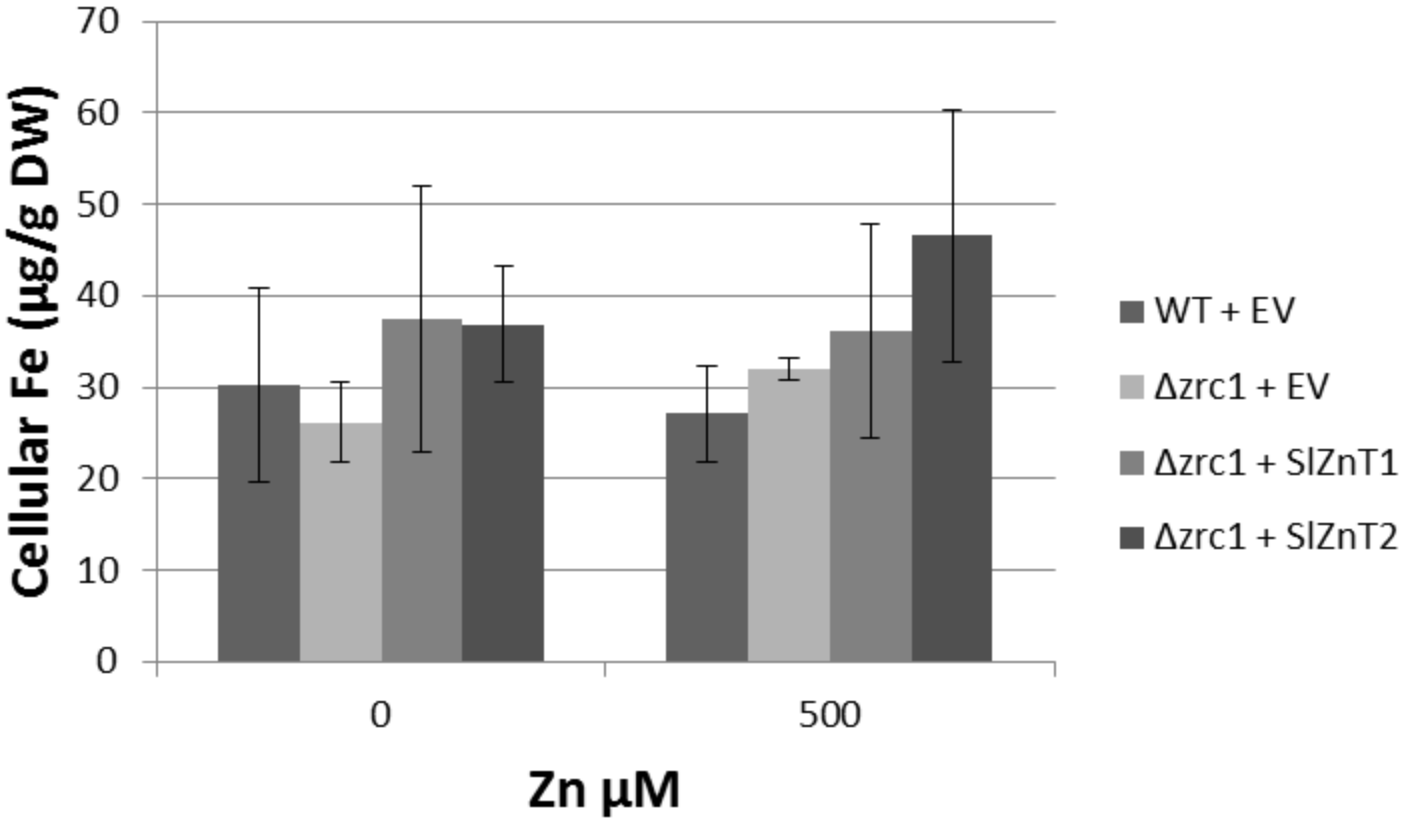
70
60
50
40
30
20
10
0
Cellular Fe (µg/g DW)
0
500
Zn µM
WT + EV
Δzrc1 + EV
Δzrc1 + SlZnT1
Δzrc1 + SlZnT2

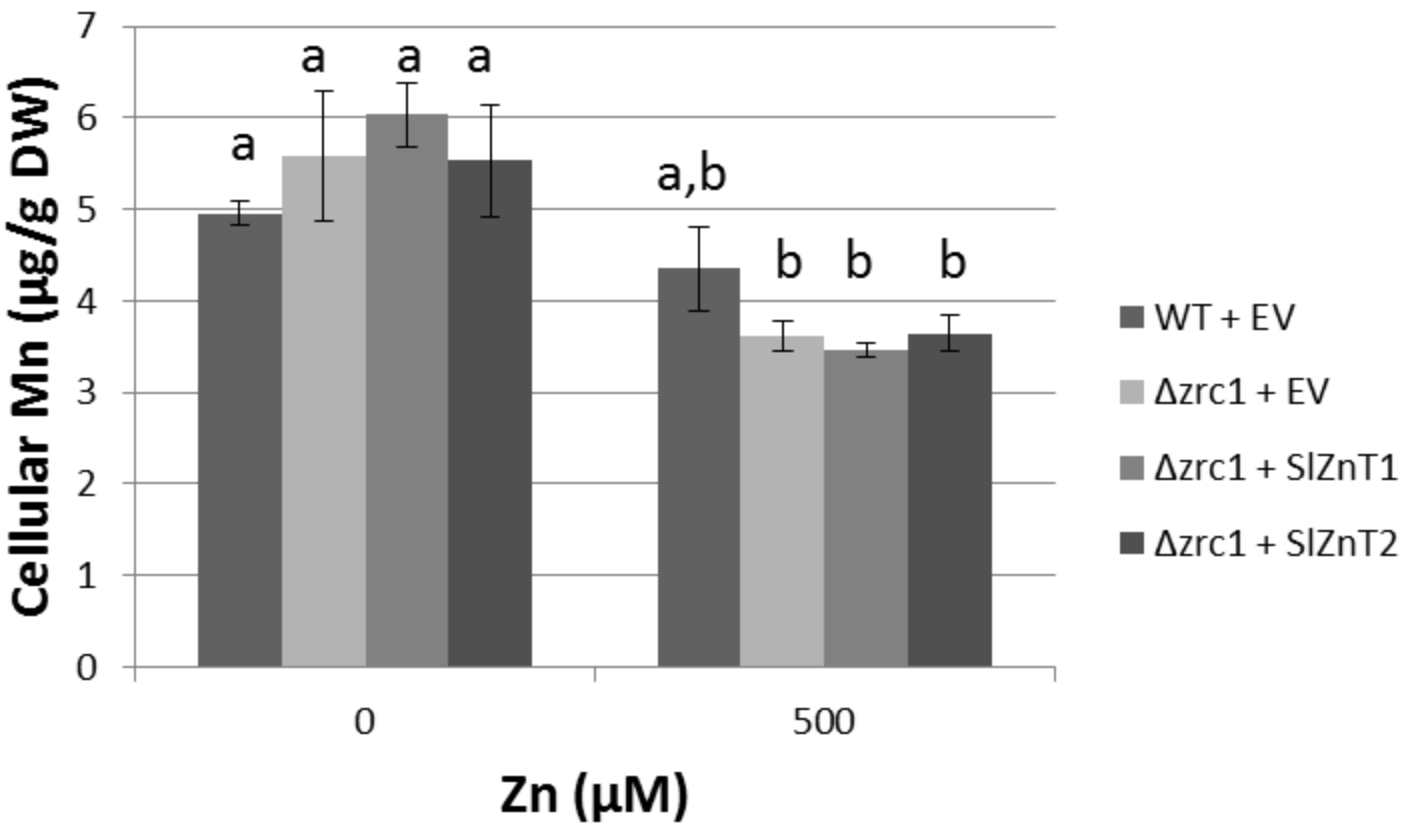
7
6
5
4
3
2
1
0
Cellular Mn (µg/g DW)
a
a
a
a
a,b
b
b
b
0
500
Zn (µM)
WT + EV
Δzrc1 + EV
Δzrc1 + SlZnT1
Δzrc1 + SlZnT2